Facultad
de
Ciencias

Around the 125 GeV light Higgs boson mass in the MSSM: predictions for the W boson mass

(Masa del bosón de Higgs ligero en torno a 125 GeV en el MSSM: predicciones para la masa del bosón W)

Trabajo de Fin de Máster
para acceder al

MÁSTER EN FÍSICA, INSTRUMENTACIÓN Y MEDIO AMBIENTE

Autor: Unai De Miguel Sárraga

Director: Sven Heinemeyer

Enero - 2019

Dedication

A los que siempre han estado ahí, cerca o lejos, apoyándome. Todo lo que soy es gracias a vosotros.

En especial a mi abuelo, una de las personas más fuertes y luchadoras que conozco. Mi mayor referente y el mayor seguidor de todo lo que hago.

También va por tí, Zor. Siempre conmigo.

Acknowledgements

Es difícil explicar con palabras todo lo agradecido que me siento del constante cariño y apoyo que he recibido de amigos, familiares, profesores,... durante estos años. Seguramente me quede corto o no sepa expresarlo bien, pero intentaré hacerlo lo mejor que sé.

Gracias a Jose Luis por despertar mi interés por la Ciencia y ser el detonante que me empujó a querer convertirme en físico. Me diste "la base" sobre la que cada día doy mis pasos.

Gracias a Alicia por descubrime este apasionante mundo que se esconde tras la Física de partículas y a Sven por enseñarme el futuro de ésta con el tutelaje y desarrollo de este trabajo.

Gracias a Paco y Julio por sus lecciones, consejos, reprimendas (sobre todo Julio, bien merecidas) y atención hacia mí, tanto en lo académico como lo personal. Sin ello, tanto este trabajo como mi forma de trabajar serían completamente distintas.

Gracias a mis compañeros del Bm. Colindres por hacer de mi hobbie mi pasión, ayudarme a desconectar y hacer todo esto más llevadero. Siempre os lo digo: no sois solo mi equipo, sois mi familia.

Gracias a mis compañeros físicos (y algún que otro físico-matemático) por hacer más llevadero este camino. Andrés, Cris, Raquel, Celia, Agustín, Javi, Pablo, Eli, Marina,... gracias por estar ahí. En especial a Elena (Elena-dela) y Fer (el puto Fer), este año no hubiera sido lo mismo sin vosotros. Las risas, los jueves de Sibaritas, el bullying a Cris (Cris te queremos). No sé, sois capaces de hacer de lo cotidiano algo especial.

Gracias a Sonia por soportarme cada día (hasta yo sé que no es fácil). Por aguantar mis tonterías y mis rayadas; mis constantes "No podemos quedar que tengo que estudiar". Gracias por aparecer cuando más difícil estaba todo. Ojalá pudiera expresar todo lo afortunado que me siento por tenerte a mi lado y agradecerte todo lo que me has enseñado. Gracias por todo lo que me transmites con una sonrisa o una mirada. Te quiero.

Gracias a mi familia por haberme acompañado y apoyado siempre durante estos años. En especial a mi madre, la que más ha sufrido conmigo pero, también, la que más ha celebrado (y llorado) todo lo que he conseguido hasta ahora. Porque ella puede decir que está orgullosa de mí en muchos aspectos, pero yo de ella lo estoy en todos. Tampoco quiero olvidarme de tí, Zor (Zorín), y de tu incansable compañia. La primera página de este trabajo la escribí contigo en mi regazo. Siempre conmigo.

Abstract

In the present work, we shall expose a general overview of the Standard Model (SM) and a brief introduction of Supersymmetry (SUSY). With these ideas, we shall set the bases on which the Minimal Supersymmetric Standard Model (MSSM) is developed. The MSSM parameter space has more than 100 free parameters but it can be constrained according to experimental evidences.
In order to do so, we shall a numerical analysis of the dependence of the mass of the Higgs boson and W boson in that supersymmetric model. First, we find ranges of free MSSM parameters that provide the mass of the light Higgs boson in the MSSM h^0 about 125 GeV i.e. that are in agreement with the mass of the Higgs boson discovered by CMS and ATLAS in 2012. Afterwards, we study the effect of these free MSSM parameters in the prediction of the W boson mass m_W. In particular, large differences between the MSSM and the SM prediction of the mass of W boson are sought in these ranges of free parameters. Finally, in agreement with these differences, we discuss how the MSSM parameter space could be constrained by (future) precision measurements of m_W.

Keywords: Supersymmetry, Standard Model, Minimal Supersymmetric Standard Model, Higgs boson, W boson, Free parameters, FeynHiggs

Resumen

En este trabajo, se expone una visión general del Modelo Estándar (SM) y una breve introducción de Supersimetría (SUSY). Con estas ideas, se darán las bases en las cuales se desarrolla el Modelo Estándar Mínimo Supersimétrico (MSSM). El espacio de parámetros del MSSM lo componen más de 100 parámetros libres los cuales pueden ser acotados de acuerdo a evidencias experimentales.
Para ello, se realiza un análisis numérico de la dependencia de la masa del bosón de Higgs y del bosón W en este modelo supersimétrico. Primero, se hallan los rangos de los parámetros libres del MSSM que proporcionan una masa del bosón de Higgs ligero del MSSM h^0 alrededor de 125 GeV, es decir, que esté de acuerdo con la masa del bosón de Higgs descubierto por CMS y ATLAS en 2012. Después, se estudia el efecto de estos parámetros libres del MSSM en la predicción de la masa del bosón W m_W. En particular, se buscan grandes diferencias entre las predicciones del MSSM y del SM para la masa del bosón W. Finalmente, de acuerdo con estas diferencias, se discute cómo acotar el espacio de parámetros del MSSM en base a (futuras) medidas precisas para m_W.

Palabras clave: Supersimetría, Modelo Estándar, Modelo Estándar Mínimo Supersimétrico, Bosón de Higgs, Bosón W, Parámetros libres, FeynHiggs

Contents

1 Introduction

Nowadays, the Standard Model (SM) of particle physics is (besides General Relativity) the most important theory that we have because it includes all that know about sub-atomic particles and their interactions. Moreover, this theory predicts the existence of a scalar particle called Higgs boson, which was confirmed by CMS [1] and ATLAS [2] (LHC experiments) on 4 July 2012. This discovery closed the particle content of the SM but open new frontiers for understanding it.

Additionally, the SM is not considered as a complete theory of fundamental interactions since, although it has numerous successes and a huge experimental prediction, there are some problems (or features) that this theory is not able to explain. Thus, the discovery of the Higgs boson also opens new frontiers to theories beyond the Standard Model (BSM).

This work focuses on the Minimal Supersymmetric Standard Model (MSSM) [3–5], a well motivated BSM theory. In particular, this model is the minimal extension to the SM that includes Supersymmetry (SUSY) [6] that is a symmetry of nature that proposes a relationship between bosonic and fermionic degrees of freedom, i.e. it predicts the existence of new particles called superpartners.

The main reason to focus on the MSSM is because it solves many SM problems (The MSSM has a candidate for Dark matter, it solves the problem of the stability of the mass of the Higgs boson with respect to quantum corrections, the gauge couplings unify at the GUT-scale,...). However, it is important to highlight that, unlike the SM, the MSSM predicts the existence of five Higgs bosons, these are:

- Three neutral bosons: light Higgs boson h^0 ($\mathcal{CP}$-even) and two heavy Higgs boson H^0 ($\mathcal{CP}$-even) and A^0 ($\mathcal{CP}$-odd). The mass of the light $\mathcal{CP}$-even Higgs boson can be calculated in terms of the other model parameters
- Two charged bosons: positive H^+ and negative H^- charged Higgs boson.

On the one side, it is important to say that, at this time, there is no experimental evidence to support the MSSM (and SUSY) yet [7, 8]. Nevertheless, there is no experimental evidence that contradicts the existence of SUSY.

On the other side, it is possible to put limits on the values of the free parameters of the model that are achieved from experimental observations. So, it is possible to obtain ranges of the values of the parameters that are not against to experimental observations.

In this work will give a general overview of the SM and a brief introduction of SUSY. With these ideas, we can explain the bases on which the MSSM is developed. After this,

we will do a numerical study of the dependence of the mass of the Higgs boson and W boson in that supersymmetric model. That analysis will have two parts:

- It is studied the dependence of the mass of h^0 with parameters of the MSSM. As explained below, it is possible to link the MSSM light Higgs boson with the Higgs boson discovered by CMS and ATLAS in 2012, whose mass is $m_H^{\text{exp}} = (125.09 \pm 0.16)$ GeV [9]. So, this part focuses on varying a set of MSSM parameters in order to get that the mass of h^0 (the m_{h^0} is predicted in terms of free MSSM parameters) is close to 125 GeV i.e. find ranges of free parameters that are in agreement with $m_{h^0} = (125 \pm 3)$ GeV (the ± 3 GeV is because of the theory uncertainty [10]).
- Within this allowed region, we study the effect of these free MSSM parameters in the prediction of the W boson mass m_W^{MSSM}, which experimental value is $m_W^{\text{exp}} = (80.379 \pm 0.013)$ GeV [11]. So, this part analyses the dependence of m_W^{MSSM} within the allowed parameter space. We show how much m_W^{MSSM} can still deviate from the SM predictions m_W^{SM}. We discuss how the MSSM parameter space could be constrained by (future) precision measurements of m_W.

1.1 Natural units

In this work we shall use the typical system of units used in particle physics. It is known as natural units where the fundamental constants are $\hbar$ (the unit of action in quantum mechanics, $\hbar = 1.055 \cdot 10^{-34}$ J s), c (the speed of light in vacuum, $c = 2.998 \cdot 10^8$ m s^{-1}) and the mass of the particles are given in energy units GeV (1 GeV $= 1 \cdot 10^9$ eV $= 1.602 \cdot 10^{-10}$ J).

On the one hand, using this system, all physics quantities are expressed as powers of GeV as it is shown in Tab. 1.1.

Quantity	Natural units	$\hbar = c = 1$
Mass	GeV / c^2	GeV
Momentum	GeV / c	GeV
Energy	GeV	GeV
Time	(GeV / $\hbar$)$^{-1}$	GeV^{-1}

Table 1: Physics quantities and their units using natural units.

On the other hand, in order to simplifying algebraic expressions (as we can see in Eq. (1), [12]), this system introduces a subtle but important change: the physics constants $\hbar$ and c take the same value $\hbar = c = 1$,

$$E^2 = p^2c^2 + m^2c^4 \longrightarrow E^2 = p^2 + m^2. \tag{1}$$

Moreover, we also used Heaviside-Lorentz units with the purpose of simplifying the equations of classical electromagnetism [12]. In this way, the relationship between fine structure constant α_e and the electron charge is

$$\alpha_e = \frac{e^2}{4\pi} \approx \frac{1}{137}. \tag{2}$$

1.2 The Standard Model formalism

Once we have defined the system of units, we going to expose a brief review of the most important properties of the fermion fields in order to introduce elements that we will be used in the next sections. Firstly, it is important to remark when we refer to Lagrangian $\mathcal{L}$ in the text we will refer to Lagrangian density. The link between "real" Lagrangian L and $\mathcal{L}$ is given by

$$L = \int \mathcal{L}\, d^4x. \tag{3}$$

On the other hand, the fermions in the SM (see Fig. 1) are described by Dirac fermions thus they are four-vector quantum fields Ψ (it also know as Dirac spinors) whose description is given by the Dirac Lagrangian as follow [12]

$$\mathcal{L}_{\text{Dirac}} = i\bar{\Psi}\gamma^\mu\partial_\mu\Psi - m\bar{\Psi}\Psi, \tag{4}$$

being $\bar{\Psi} \equiv \Psi^\dagger\gamma^0$ and γ^μ are the gamma matrices (Eq.(4) and Eq.(9) are different representations of the same Lagrangian). The form of those gamma matrices (with $\mu = 1, 2, 3, 4$) are

$$\gamma^0 = \begin{pmatrix} I & 0 \\ 0 & -I \end{pmatrix}, \qquad \gamma^k = \begin{pmatrix} 0 & \sigma_k \\ -\sigma_k & 0 \end{pmatrix}, \qquad \gamma^5 = \begin{pmatrix} 0 & I \\ I & 0 \end{pmatrix}, \tag{5}$$

being I the identity matrix, $\gamma^5 \equiv i\gamma^0\gamma^1\gamma^2\gamma^3$ and σ_k the Pauli matrices define as

$$\sigma_1 = \begin{pmatrix} 0 & 1 \\ 1 & 0 \end{pmatrix}, \qquad \sigma_2 = \begin{pmatrix} 0 & -i \\ i & 0 \end{pmatrix}, \qquad \sigma_3 = \begin{pmatrix} 1 & 0 \\ 0 & -1 \end{pmatrix}. \tag{6}$$

Finally, we define the projector operators as

$$P_L = \tfrac{1}{2}(1 - \gamma^5), \qquad P_R = \tfrac{1}{2}(1 + \gamma^5). \tag{7}$$

Based on these operators, it is possible to redefine the Dirac spinors as

$$\Psi = P_L\Psi + P_R\Psi = \Psi_L + \Psi_R, \tag{8}$$

where they are called left-handed and right-handed chiralities, respectively.

2 Theoretical basis

Particle physics is a branch of physics whose purpose is to answer a transcendental question: "what are we made of?" i.e. to know what are the smallest constituents of Universe and to understand how they interact with each other. These constituents are called elementary particles and their interactions are called forces [12].

To know what are the elementary particles that constitute matter has been one of the great goals of the science since the beginning of knowledge. Until the end of the 19th century, physics considered that atoms were these fundamental constituents. This was believed until 1911 when Ernest Rutherford, from a correct analysis of the Geiger-Marsden experiments, concluded that atoms were composed of a charge positive nuclei with the electrons around them [13]. Years later, in the early 20th century, with similar Geiger-Marsden experiments, it was discovered that nuclei are composed of two types of particles: protons (Ernest Rutherford in 1919 [14]) and neutrons (James Chadwick in 1932 [15]), being these particles called nucleons. In 1969, from deep inelastic scattering experiments, it was discovered that nucleons are not elementary since they are composed of a new type of particle: quarks [16, 17]. At the current time, all of matter that we can see are composed of quarks (quark u and quark d) and electrons, being these particles considered as elementary particles.

On the other hand, as mentioned earlier, particle physics also studies the interaction between particles. In the nature exists four fundamental forces where three of them are described by a Quantum Field Theory (QFT) [18] (the electromagnetism, the weak and the strong interaction) where the interaction between particles of matter, for example the electromagnetism, are mediated by the exchange of photons. In short, the interactions are described by the exchange of force-carrying particles where these are called gauge bosons. The four fundamental forces and their respective gauge bosons are shown in Tab. 2

Interaction	Gauge bosons	Mass / GeV
Electromagnetic	photon $\longrightarrow \gamma$	0
Weak	W boson $\longrightarrow W^{\pm}$	80.4
	Z boson $\longrightarrow Z^0$	91.2
Strong	gluon $\longrightarrow g$	0
Gravitational	graviton (hypothetical) $\longrightarrow G$	$< 6 \cdot 10^{-41}$

Table 2: The four fundamental forces of nature, the force-carrying particles and their respective masses [19].

Today, the only theory that successfully describes the behavior of these fundamental particles is the Standard Model (SM) of particle physics. It describes very accurately the weak, the strong and the electromagnetic interactions but it does not include the gravitational interaction. In this section we will briefly discuss the basics of this theory and some problems (or features) that this theory can not answer.

2.1 The Standard Model

At the current time, the SM of particle physics (SM) is the most powerful theory at experimental level which also predicts the existence of a set of particles which have been discovered. In addition to that, it is the only theory of physics that provides a successful description of three of the four fundamental forces of nature (the strong, the weak and the electromagnetic interactions). However, as we will see in Sec. 2.1.6, it is important to highlight that the SM presents some imperfections that this model is not able to solve. Despite this, the SM is undoubtedly the best theory that provides a description of behaviour of, until now, the considered fundamental particles.

2.1.1 Particle content of the SM

The SM contains a large number of particles which present different characteristics and different ways to interacting. A good property to classify the particles is their spin. Those particles that have spin 1/2 (half-integer spin) are called fermions and those that have integer spin are known as bosons. The fermions f are also called matter particles and they have two degrees of freedom expressed in terms of their chirality i.e. left-handed and right-handed chirality (f_L, f_R) with exception of neutrinos which have only been observed with left-handed chirality [20]. There are two types of fermions: quarks and leptons. The quarks are the constituents of particles like protons and neutrons and these elementary particles are the only ones that experiences the strong interaction plus the rest of interactions[1]. On the other hand, there are two types of leptons: the neutral leptons (or neutrinos), that only experiences the weak interaction, and the charged leptons (or electron-like leptons), that feel both weak and electromagnetic interactions. Moreover, the fermions can be organized in families of particles which have similar properties except their masses. According this property, it is possible to define three generations of particles: the first generation (or the lightest generation) corresponds to the ordinary or "everyday"

[1] Although the SM is not able to explain gravitation and, today, it is not understood the behaviour of subatomic particles through this force, it is assumed that all particles feel the graviational interaction.

matter and the second and third generation (each heavier than the previous) correspond to exotic matter. All the fermions are summarized in Fig. 1.

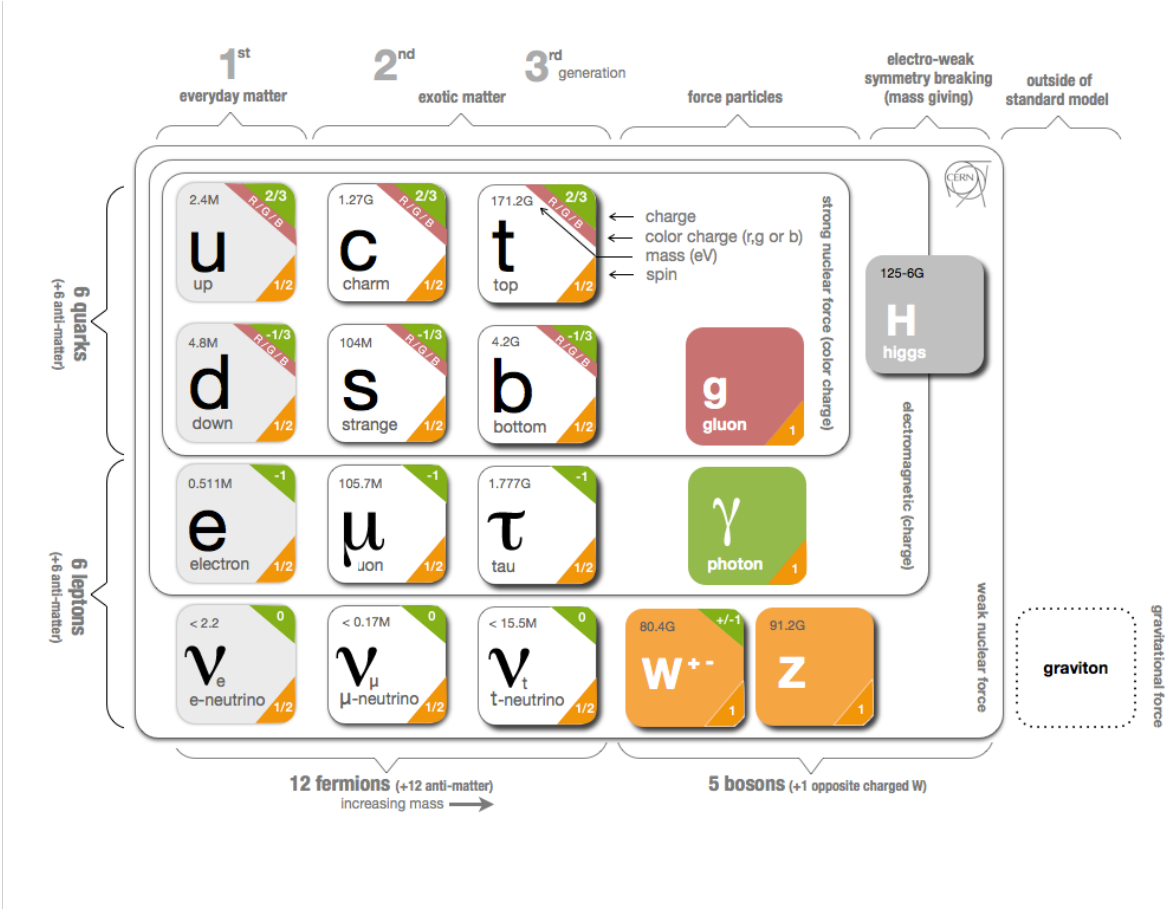

Figure 1: The particle content of the Standard Model of particle physics with their respective masses plus the gravitational force and his hypothetical force-carrying particle: the graviton [21].

As we mencioned previously, the particles with integer spin are called bosons. In the SM (in agreement with the experimental discoveries) exits two types of bosons: the gauge bosons and the Higgs boson. The gauge bosons[2] have spin 1 and these are the carrier particles of the fundamental interactions i.e. the interaction between particles is produced

[2]All discovered gauge bosons have spin 1 and, in addition to that, they also called as vector bosons.

by the exchange of gauge bosons. The carrier particles of the electromagnetic interaction are the photons γ, the carrier particles of the strong interaction are the gluons g and the mediators of the weak interaction are the neutral Z boson Z^0 and the charged W bosons $W^{\pm}$. On the other hand, the particle with spin 0 are known as Higgs boson[3] which exists as a consequence of the Brout-Englert-Higgs mechanism [22, 23] which is essential to understand how matter particles and gauge bosons acquire their masses. Finally, all the bosons are also summarized in Fig. 1.

2.1.2 Gauge symmetries

Most physical theories are formulated in the framework of the Quantum Field Theory (QFT) which, in short, is a theoretical framework where the quantum mechanics and special relativity are united. Moreover, it includes the idea of field which covers all the space-time where the gauge bosons mentioned in Sec. 2.1.1 would be excitations of the respective fields [18]. Some field theories are based on gauge theories which, shortly, the Lagrangian $\mathcal{L}$ is invariant under certain transformations of symmetry being the symmetries that make invariant the Lagrangian called gauge symmetries. Moreover, these symmetries can be defined as local symmetries if these depend on the point of the space-time.

In the next section, we describe the construction of the Lagrangian of quantum electrodynamics theory in order to give a better understanding of these concepts.

2.1.3 Quantum electrodynamics

The theory of quantum electrodynamics (QED) is the most simple gauge theory that was developed and it describes the interaction of charged particles (with spin 1/2) with the electromagnetic field. In this section, we will start with the Lagrangian of free fermionic particle in order to build the Lagrangian of QED. It is important to say that many of the following results, concepts and calculations are based on [12].

The Dirac Lagrangian for a fermionic charged particle, e.g. an electron, has the form

$$\mathcal{L}_{\text{Dirac}} = \bar{\Psi}(x)(i\gamma^{\mu}\partial_{\mu} - m)\Psi(x), \tag{9}$$

where Ψ are the Dirac spinors, $\bar{\Psi} \equiv \Psi^{\dagger}\gamma^0$ and γ^{μ} are the Dirac matrices.

[3]The Higgs boson has spin 0 thus it is a scalar boson.

Now, we apply to Ψ a gauge transformation whose form is

$$\begin{aligned} \Psi(x) &\longrightarrow \Psi'(x) = e^{i\alpha}\Psi(x), \\ \bar{\Psi}(x) &\longrightarrow \bar{\Psi}'(x) = e^{-i\alpha}\bar{\Psi}(x), \end{aligned} \tag{10}$$

where $\alpha \in \mathbb{R}$. As $\mathcal{L}_{\text{Dirac}}$ does not change under a phase transformation, it is said that Eq.(9) has a $U(1)$ global symmetry[4]. However, we are interested in $U(1)$ being a local symmetry then it is necessary to change the parameter α as function to space-time i.e. to define $\alpha \equiv \alpha(x)$. It is evident that, as we can see in Eq.(11), the Dirac Lagrangian does not remain invariant under this transformation.

$$\begin{aligned} \mathcal{L}_{\text{Dirac}} \longrightarrow \mathcal{L}'_{\text{Dirac}} &= (e^{-i\alpha(x)})\bar{\Psi}(x)(i\gamma^\mu\partial_\mu - m)(e^{i\alpha(x)})\Psi(x) = \\ &= \cancel{(e^{-i\alpha(x)})}\bar{\Psi}(x)(i\gamma^\mu\partial_\mu - m)\cancel{(e^{i\alpha(x)})}\Psi(x) + \\ &+ \cancel{(e^{-i\alpha(x)})}\bar{\Psi}(x)(i\gamma^\mu\left[i\partial_\mu\alpha(x)\right])\cancel{(e^{i\alpha(x)})}\Psi(x) \\ \implies \mathcal{L}'_{\text{Dirac}} &= \bar{\Psi}(x)(i\gamma^\mu\partial_\mu - m)\Psi(x) \; - \; \bar{\Psi}(x)\gamma^\mu\left[\partial_\mu\alpha(x)\right]\Psi(x) \neq \mathcal{L}_{\text{Dirac}}. \end{aligned} \tag{11}$$

In order to delete the extra term in Eq.(11) and, with that, get a Lagrangian invariant under $U(1)$ local symmetry it is necessary to add a new vector field $A_\mu(x)$ which is a gauge field associated to the photon. This new field changes as

$$A_\mu(x) \longrightarrow A'_\mu(x) = A_\mu(x) + \frac{1}{q}\partial_\mu\alpha(x), \tag{12}$$

where q is the electric charge. Besides that, it is required to redefine the derivate as

$$\partial_\mu \longrightarrow D_\mu \equiv \partial_\mu - iqA_\mu(x). \tag{13}$$

Then, if we replace ∂_μ with D_μ in Eq.(9), we will a new Dirac Lagrangian like follow

$$\mathcal{L}_{\text{Dirac}} = \bar{\Psi}(x)(i\gamma^\mu D_\mu - m)\Psi(x) = \bar{\Psi}(x)(i\gamma^\mu\partial_\mu - m)\Psi(x) + q\bar{\Psi}(x)\gamma^\mu\Psi(x)A_\mu(x) \tag{14}$$

where if we apply a $U(1)$ local transformations, we have

$$\begin{aligned} \mathcal{L}_{\text{Dirac}} \longrightarrow \mathcal{L}'_{\text{Dirac}} &= \bar{\Psi}(x)(i\gamma^\mu\partial_\mu - m)\Psi(x) \; - \; \cancel{\bar{\Psi}(x)\gamma^\mu\left[\partial_\mu\alpha(x)\right]\Psi(x)} + \\ &+ \cancel{\bar{\Psi}(x)\gamma^\mu\left[\partial_\mu\alpha(x)\right]\Psi(x)} + q\bar{\Psi}(x)\gamma^\mu\Psi(x)A_\mu(x) \\ \implies \mathcal{L}'_{\text{Dirac}} &= \bar{\Psi}(x)(i\gamma^\mu\partial_\mu - m)\Psi(x) + q\bar{\Psi}(x)\gamma^\mu\Psi(x)A_\mu(x) = \mathcal{L}_{\text{Dirac}}. \end{aligned} \tag{15}$$

[4]The global group $U(1)$ is composed for all complex numbers with absolute value equal to 1 [24].

which, as it has been demonstrated, remains invariant under $U(1)$ local transformations. At last, including in Eq.(15) the kinetic term for the massless spin 1 field (from Maxwell's equations Lagrangian in the vacuum) the QED Lagrangian can be written as

$$\mathcal{L}_{\text{QED}} = -\frac{1}{4}F_{\mu\nu}F^{\mu\nu} - j^{\mu}A_{\mu} + \bar{\Psi}(x)(i\gamma^{\mu}\partial_{\mu} - m)\Psi(x), \tag{16}$$

where $j^{\mu} = -q\bar{\Psi}(x)\gamma^{\mu}\Psi(x)$ is the four-vector current density, $F_{\mu\nu} = \partial_{\mu}A_{\nu} - \partial_{\nu}A_{\mu}$ and the $F_{\mu\nu}F^{\mu\nu}$ term is also invariant under $U(1)$ local transformations.

Finally, it is important to emphasize the fact that we have required a local gauge symmetry in the Lagrangian of our system it has led us to build a Lagrangian description of the electromagnetic interaction.

2.1.4 Electroweak interaction

In the same way that the SM describes QED as $U(1)$ gauge local symmetry, it explains the weak interaction as $SU(2)_L$ gauge local invariance where the L subindex is due to this symmetry only affects left-handed fermions. Under this interaction, the fermions "charge" is called weak isospin I. According to the definition of I, it is possible to write the wavefunction φ in terms of the isospin doublets and singlets. The isospin doublet for left-handed fermions has the expression

$$\varphi_L = \begin{pmatrix} \nu_e \\ e^- \end{pmatrix}_L, \tag{17}$$

for the first generation of leptons. As we can see in Eq.(17) φ_L is a doublet that has total weak isospin I equal to $1/2$ and the third component of weak isospin $I_L^{(3)}$ is equal to $+1/2$ for ν_{eL} and equal to $-1/2$ for e_L. On the other hand, for right-handed fermions, the weak isospin is a singlet $\varphi_R = e_R^-$ whose value $I_R = I_R^{(3)} = 0$. In addition to that, due to the presence of this isospin, it is neccesary the existence to three weak current one for each gauge fields $W_{\mu}^{(k)}$ (with $k = 1, 2, 3$) i.e. the gauge fields $W_{\mu}^{(k)}$ are the fields associate to $SU(2)_L$ gauge local group. At last, combinations of $W_{\mu}^{(1)}$ and $W_{\mu}^{(2)}$ give rise to weak charged-currents which are associated to $W^{\pm}$ bosons.

However, we have a weak neutral-current that is not yet possible to identify with the Z^0 boson. Starting from this, we have γ boson gauge associates a A_{μ} gauge field and Z^0 boson gauge associates a Z_{μ} gauge field (we have not yet defined it), both are neutral. Nevertheless, the $U(1)$ local group does not couple with the $SU(2)_L$. Starting from this, Glashow, Salam and Weinberg (GSW) [25–27] build a new model that explains the weak and electromagnetic interaction as a only one force: the electroweak interaction (EW).

First, GSW electroweak model changes the $U(1)$ local gauge symmetry for $U(1)_Y$, where Y is called hypercharge which couples with a new gauge field B_μ. Moreover, the Y is related with electric charge and third component of weak isospin $I^{(3)}$. The Y can be identified as

$$Y = 2\left(Q - I^{(3)}\right), \tag{18}$$

where this expression is known as Gell-Mann-Nishijima formula [28,29]. Now, the A_μ and Z_μ gauge fields are witten as lineal combinations of the $W_\mu^{(3)}$ and B_μ as follow in this unified model

$$\begin{aligned} A_\mu &= +B_\mu \cos\theta_W + W_\mu^{(3)} \sin\theta_W, \\ Z_\mu &= -B_\mu \sin\theta_W + W_\mu^{(3)} \cos\theta_W, \end{aligned} \tag{19}$$

where θ_W is the weak mixing angle. Finally, we will build the simplest electroweak Lagrangian $\mathcal{L}_{\text{EW}}$ which is invariant under $SU(2)_L \times U(1)_Y$. First, we define the isospin doublets left-handed and singlets right-handed as

$$\begin{gathered} \chi_e = \begin{pmatrix} \nu_{eL} \\ e_L \end{pmatrix}, \quad \chi_u = \begin{pmatrix} u_L \\ d_L \end{pmatrix}, \\ \psi_e = e_R, \qquad \psi_u = \begin{Bmatrix} u_R \\ d_R \end{Bmatrix}, \end{gathered} \tag{20}$$

for the first generation of fermions. According to Eqs.(18 and 20) the isospin doublets have the same Y_L value and the isospin singlets have $Y_R \neq 0$ which involves that, as expected, the right-handed fermions couple with B_μ gauge field. In addition to that, it is necessary to redefine the derivates as follows

$$D_{L\mu} = \partial_\mu - ig_2 \frac{\sigma_k}{2} W_\mu^{(k)} + ig_1 \frac{Y_L}{2} B_\mu, \qquad D_{R\mu} = \partial_\mu + ig_1 \frac{Y_R}{2} B_\mu \tag{21}$$

where g_2 and g_1 are the gauge couplings of weak isospin (or weak mixing) and hypercharge, respectively, being both couplings relate to the electron charge by

$$e = \frac{g_1 g_2}{\sqrt{g_1^2 + g_2^2}}, \tag{22}$$

and both couplings are related to the weak mixing angle by

$$e = g_2 \sin\theta_W = g_1 \cos\theta_W. \tag{23}$$

This relation between both couplings allows us to define the gauge fields in Eq.(19) as follows

$$\begin{aligned} A_\mu &= \frac{1}{\sqrt{g_1^2 + g_2^2}} (+g_1 B_\mu + g_2 W_\mu^{(3)}), \\ Z_\mu &= \frac{1}{\sqrt{g_1^2 + g_2^2}} (-g_1 B_\mu + g_2 W_\mu^{(3)}), \end{aligned} \tag{24}$$

Based on all of the above, the simplest electroweak Lagrangian $\mathcal{L}$ can be written as

$$\mathcal{L}_{\rm EW} = \sum_f \left(\bar{\chi}_f i\gamma^\mu D_{L\mu}\chi_f + \bar{\psi}_f i\gamma^\mu D_{R\mu}\psi_f\right) - \frac{1}{4}W^{(k)}_{\mu\nu}W^{(k)\mu\nu} - \frac{1}{4}B_{\mu\nu}B^{\mu\nu}, \tag{25}$$

where the χ_f and ψ_f refer to each doblets and singlets of fermions and it has been included the kinetic terms associate to B_μ and $W^{(k)}_\mu$ gauge fields. However, the main problem of this electroweak Lagrangian is there are not mass terms for fermions and bosons and, as we know experimentally, all the particles (except the photon γ) involved in the electroweak interaction have mass. So, it is necessary that appear mass terms in Eq.(25), specially with the form

$$-m_f\bar{\Psi}_f\Psi_f, \tag{26}$$

for fermions and with the form

$$+\frac{1}{2}m_X^2 X_\mu X^\mu, \tag{27}$$

for bosons, being X_μ a gauge field. If we include these terms in Eq.(25), $\mathcal{L}_{\rm EW}$ will be not invariant under $SU(2)_L \times U(1)_Y$ transformations thus it is necessary to find a mechanism to provide mass to fermions and the electroweak bosons. The way in which these particles get their mass through the Brout-Englert-Higgs mechanism [22, 23], it also well known as the Higgs mechanism[5].

2.1.5 The Higgs mechanism

In the SM, particles acquire their mass through their interaction with the Higgs field which is a quantum field that permeates all the space. The way that mechanism gives mass to the electroweak bosons is due to break spontaneously the electroweak symmetry. For this it is necessary to include in Eq.(25) the corresponding new contribution of this mechanism which form is

$$\mathcal{L}_H = (D_{L\mu}\phi(x))^\dagger D_L^\mu \phi(x) - V(\phi(x)), \tag{28}$$

where $\phi(x)$ is a complex doublet and it is well known as Higgs doublet which can be written as

$$\phi(x) = \begin{pmatrix} \phi^+(x) \\ \phi^0(x) \end{pmatrix}, \tag{29}$$

where ϕ^+ and ϕ^0 have two components each one therefore the Higgs doublet contains four degree of freedom. Moreover, the scalar potential $V(\phi(x))$ is given by

$$V(\phi(x)) = -\mu^2_{\rm SM}\phi^\dagger\phi + \frac{\lambda}{4}(\phi^\dagger\phi)^2 = -\mu^2_{\rm SM}|\phi|^2 + \frac{\lambda}{4}|\phi|^4. \tag{30}$$

[5]From now on, we will refer to the Brout-Englert-Higgs mechanism as the Higgs mechanism.

The most important feature of this potential is it has a non-zero minimum when $(\phi^\dagger\phi)_0 = |\phi|_0^2 = \frac{2\mu_{\rm SM}^2}{\lambda} \equiv \frac{v^2}{2}$ where v is the vacuum expectation value (vev). This potential has that non-zero minimun when $\mu_{\rm SM}^2 > 0$, being this feature which makes that the Higgs mechanism breaks the EW symmetry. Then, we can choose the vev for the Higgs field as

$$|\phi|_0 = \frac{v}{\sqrt{2}} \Longrightarrow \quad \phi_0 = \frac{1}{\sqrt{2}} \begin{pmatrix} 0 \\ v \end{pmatrix}, \tag{31}$$

and the Higgs doublet in Eq.(29) can be expanded about this minimum as follows

$$\phi(x) = \begin{pmatrix} \xi_1(x) + i\xi_2(x) \\ v + \eta(x) + i\xi_4(x) \end{pmatrix}, \tag{32}$$

where $\eta(x)$ is a scalar field and ξ_1, ξ_2 and ξ_3 are fields associated with non-physical Goldstone bosons. If we write the Higgs doublet $\phi(x)$ as gauge unitary[6], we will obtain $\phi(x)$ as follows

$$\phi(x) = \begin{pmatrix} 0 \\ v + H(x) \end{pmatrix}, \tag{33}$$

where $H(x)$ is a physical field that is associated with the Higgs boson. Based on the last result, we can understand that one ϕ degree of freedom turns into a physical Higgs boson. As we will see, the other three degrees of freedom are used to give mass of the $W^\pm$, Z^0 gauge bosons. If we substitute the last result in $\mathcal{L}_H$ we will get terms which correspond with mass terms of the EW bosons. We call at the part of $\mathcal{L}_H$ that only considers the EW mass terms as $\mathcal{L}_{\rm EWmasses}$, whose form is

$$\mathcal{L}_{\rm EWmasses} = \frac{v^2 g_2^2}{4}\left(W_\mu^{(1)} + iW_\mu^{(2)}\right)\left(W^{(1)\mu} - iW^{(2)\mu}\right) + \frac{v^2}{4}\left(-g_1 B_\mu + g_2 W_\mu^{(3)}\right)^2, \tag{34}$$

where, at the same way to Eq.(24), it is possible to define two new fields as lineal combinantions of the $W_\mu^{(1)}$ and $W_\mu^{(2)}$ as follows

$$\begin{aligned} W_\mu^+ &= \frac{1}{\sqrt{2}}\left(W_\mu^{(1)} - iW_\mu^{(2)}\right), \\ W_\mu^- &= \frac{1}{\sqrt{2}}\left(W_\mu^{(1)} + iW_\mu^{(2)}\right), \end{aligned} \tag{35}$$

where that are the gauge fields associate to $W^\pm$ gauge bosons. Finally, if we consider the expresions in Eqs.(24 and 35) and the boson mass term given by Eq.(27) we can write $\mathcal{L}_{\rm EW\ masses}$ as

$$\mathcal{L}_{\rm EWmasses} = \frac{v^2 g_2^2}{8} W_\mu^+ W^{-\mu} + \frac{v^2}{8}(g_1^2 + g_2^2) Z_\mu Z^\mu, \tag{36}$$

[6]In short, to write the Higgs doublet as gauge unitary consists in to delete the Goldstone fields and to get a real field.

and, in consequence, we can obtain the masses of the EW bosons. The mass expressions of the EW bosons are:

$$\frac{1}{2}m_W^2 = \frac{v^2 g_2^2}{8} W_\mu^+ W^{-\mu} \Longrightarrow m_W = \frac{v g_2}{2} \tag{37}$$

for the $W^\pm$ bosons,

$$\frac{1}{2}m_Z^2 = \frac{v^2}{8}(g_1^2 + g_2^2) Z_\mu Z^\mu \Longrightarrow m_Z = v\frac{\sqrt{g_1^2 + g_2^2}}{2} = \frac{m_W}{\cos\theta_W} \tag{38}$$

for the Z^0 bosons and, as expected, that there is not mass term for the gauge field A_μ implies that its respective gauge boson (the photon γ) has no mass. Similarly, it is possible to get the fermions mass but now the fermions mass terms has the Eq.(26) form. Finally, the expression of the coupling of Higgs boson H^{SM} with fermions are:

$$\mathcal{L}_{H^{\text{SM}}\bar{f}f} = -\frac{g_2 m_f}{\sqrt{2} m_W} \bar{f} f \; H^{\text{SM}} \tag{39}$$

2.1.6 Standard Model problems

As we said at the beginning of the Sec. 2.1, the SM presents some imperfections or features that it is not able to give resolve. These flaws open new frontiers to theories beyond the Standard Model (BSM) which, keeping the structure of the SM, add new symmetries or interactions in the model which involve new particles, i.e. the BSM theories are based on the addition of new physic in the SM.

Below are shown a brief explanation to the main problems that the SM is not capable to solve.

Dark matter

The dark matter receives this name because it is a kind of matter that does not interaction with the electromagnetic radiation thus it is not possible to detect with our telescopes but we can detect its gravitational influence. Most of the scientific community accepts the existence of dark matter since there are many experimental astrophysical evidences that prove their existence [30] as the measuring of the dynamics of galaxies or gravitational lensing effect. It is true that there are alternatives to dark matter, as modified gravity [31], but they are not of able to describe the wealth of experimental data.

The experimental evidences show that dark matter must be massive and stable, without electrc charge [32]. In all the particle content of the SM does not exist a type of particle that could be a dark matter candidate, being this one of the main problems of the SM.

Grand unification

One of the goals of the theoretical physics is to get a Theory of Everything i.e. a theory that unifies the four fundamental forces of the nature. In the SM is possible to unify the electromagnetism and the weak interactions in one just force: the electroweak interaction. However, it seems that the strong interaction does not converge with the other forces in the SM. The aim is to build a theory that finds a energy scale for which the gauge couplings g_s, g_1 and g_2 (associated to strong interaction, hypercharge and weak isospin, respectively) converge to a common value. Those theories are known as Grand Unification Theories (GUT) [33] and, as we can deduce, the SM is not a theory of this type.

Hierarchy problem

In this model, the hierarchy problem is know as the problem of naturalness of the SM which is based on why the mass of the Higgs boson m_H is so far from the Planck scale [34]. In the SM, the mass of the Higgs boson receives radiative corrections from all particles with which it interacts then it would be natural for m_H to be around at the theoretical cut off, the Planck scale, being this [35]

$$M_{\text{Planck}} = \sqrt{\frac{\hbar c}{\mathrm{G}}} \simeq 10^{19}\ \text{GeV}, \tag{40}$$

where it is considered that the strength of the gravitational interaction is similar to the strength of the other forces [36]. However, we know that the Higgs boson sets the mass of the EW bosons $W^{\pm}$ and Z^0 thus the mass of the Higgs boson must be around $m_W \simeq m_Z \simeq 100$ GeV (CMS and ATLAS measured $m_H^{\text{exp}} = (125.09 \pm 0.16)$ GeV). So, the SM needs unnaturally large cancellations of contributions to m_H i.e the Higgs boson mass is another question that the SM is not capable to answer.

2.2 Supersymmetry

In the last decades, as a consequence of the problems of the SM, numerous BSM theoretical models have been developed in order to solve these flaws that the SM presents. However, among all these models, those that are based on the idea of Supersymmetry (SUSY) stand out that, as described in [37], "... it is one of the most strikingly beautiful recent ideas in Physics".

The SUSY base is sustained in the existence of new symmetry of the nature which relates bosonic and fermionic degrees of freedom i.e. for each fermionic degree of freedom

(f_L, f_R), corresponding to their chiralities, it has associated a bosonic supersymmetric degree of freedom $(\tilde{f}_L, \tilde{f}_R)$ and vice versa. In short, SUSY can be defined as a symmetry transformation $\hat{Q}$ that turns fermionic (bosonic) states into bosonic (fermionic) states as follow

$$\begin{aligned} \hat{Q} \left|\text{Fermion}\right\rangle &= \left|\text{Boson}\right\rangle, \\ \hat{Q} \left|\text{Boson}\right\rangle &= \left|\text{Fermion}\right\rangle, \end{aligned} \tag{41}$$

where the operator $\hat{Q}$ relates these two states. In addition, it is important to say that those new states will be referred as supersymmetric partners or superpartners.

As example of supersymmetric model, it is considered a particular case of the Wess-Zumino model [38] composed by a massless left-handed fermion Ψ_L with spin 1/2 and a massless boson with spin 0 defined by the complex escalar field ϕ, both without interaction between them. For the following explanation we have taken into account [38] and [39]. The system described here is defined by the Klein-Gordon Lagrangian as

$$\mathcal{L} = -\partial^\mu \phi^\dagger(x) \partial_\mu \phi(x) + i \Psi_L(x) \gamma^\mu \partial_\mu \Psi_L(x). \tag{42}$$

An infinitesimal SUSY transformation on this system should change it as follow

$$\begin{aligned} \phi(x) &\longrightarrow \phi'(x) = \phi(x) + \delta\phi(x) \\ \Psi_L(x) &\longrightarrow \Psi'_L(x) = \Psi_L(x) + \delta\Psi_L(x) \end{aligned}, \tag{43}$$

with

$$\delta\phi(x) \simeq \epsilon \Psi_L(x), \qquad \delta\Psi_L(x) \simeq \epsilon \phi(x), \tag{44}$$

where ϵ is a parameter that characterize the SUSY transformation. As we can see, this symmetry relates the scalar field ϕ with the spinor Ψ_L and vice versa. The next step would be to correctly define ϵ, $\delta\phi(x)$ and $\delta\Psi_L(x)$ in order to get that Lagrangian is invariant under this type of symmetry transformation. A complete development can be seen in [39].

In this section, a brief introduction of how to construct a SUSY Lagrangian it has been shown. Based on these ideas, in Sec. 2.3 it is exposed the Minimal Supersymmetric Standard Model which is the simplest SUSY theory constructed from the SM.

2.3 The Minimal Supersymmetric Standard Model

The minimal supersymmetric extension of the SM is the Minimal Supersymmetric Standard Model (MSSM) i.e. the MSSM is the minimal supersymmetric theory that contains

the SM. Consequently, this new model includes all the particle content of the SM plus the new superpartner particles.

As we explained before, SUSY is a symmetry that links bosonic and fermionic degrees of freedom: each bosonic degree of freedom have associated a fermionic degree of freedom and vice versa. This is the reason for the existence of new particles which are superpartners of SM particles. Moreover, notice that if SUSY is exact the superpartners must have the same mass. Since these superpartners have not been discovered, they must have a mass larger than their SM partners, i.e. SUSY is a broken symmetry [40]. According to this aspect it is necessary to include new free parameters in this theoretical model. These new parameters are called soft SUSY-breaking parameters which affect the SUSY particles in order to these do not have the same mass as the SM particles.

In the following sections we will give a brief introduction of the MSSM sectors and we will also highlight the most important free parameters in each sector.

2.3.1 The Higgs Sector of the MSSM

Within this theory, unlike the SM, it is necessary to have two complex Higgs doublets in order to give masses to up-type and down-type fermions [41]. These doublets are H_u and H_d and they have the form

$$H_u = \begin{pmatrix} H_u^+ \\ H_u^0 \end{pmatrix} \qquad H_d = \begin{pmatrix} H_d^0 \\ H_d^- \end{pmatrix}, \tag{45}$$

where H_u (H_d) couples to u-type[7] (d-type[8]) fermions i.e. complex Higgs doublets H_u and H_d give the mass of u-type and d-type fermions, respectively.

On the other hand, each component of the Higgs doublets have linked a superpartner with spin 1/2. These superpartners are called higgsinos and they have the form

$$\tilde{H}_u = \begin{pmatrix} \tilde{H}_u^+ \\ \tilde{H}_u^0 \end{pmatrix} \qquad \tilde{H}_d = \begin{pmatrix} \tilde{H}_d^0 \\ \tilde{H}_d^- \end{pmatrix}, \tag{46}$$

which are discussed in Sec. 2.3.4. Like the SM, the reason why these doublets give the mass of the rest of particles is because these doublets obtain a *vev*, called v_u and v_d for

[7] The u-type are the quarks u (up), c (charm) and t (top).

[8] The d-type fermions are the quarks d (down), s (strange) and b (bottom) and the leptons e^- (electron), μ^- (muon) and τ (tau).

H_u and H_d, respectively. Notice that v_u and v_d should not be independient, they must satisfy $\sqrt{v_u^2 + v_d^2} = v \simeq 246$ GeV. Moreover, we can define v_u and v_d as

$$v_u = v \sin\beta, \qquad v_d = v \cos\beta, \tag{47}$$

and, based on this definition, the ratio of vev is [37]

$$\tan\beta = \frac{v_u}{v_d}, \tag{48}$$

where $\tan\beta$ is a free parameter of the MSSM and, as we will see later, this is one of the most important Higgs sector parameters.

Another important free parameter of the MSSM is the higgsino mass parameter μ which appears into the scalar potential of the MSSM V_{MSSM} [39]. Inside the Higgs sector, this scalar potential of the neutral components has the form

$$\begin{aligned} V_{\text{MSSM}} = (|\mu|^2 + m_{H_u}^2)|H_u^0|^2 + (|\mu|^2 + m_{H_d}^2)|H_d^0|^2 - \\ - BH_u^0 H_d^0 - B^* H_u^{0*} H_d^{0*} + \frac{1}{8}(g^2 + g'^2)(|H_u^0|^2 - |H_d^0|^2)^2, \end{aligned} \tag{49}$$

where, as we explain later, μ also contributes in the mass of others supersymmetric particles.

The two complex Higgs doublets contain eight degrees of freedom. Like the SM, three of them are used to give mass of the gauge bosons but now we have five degrees of freedom which will turn into five physical Higgs bosons: three neutral (light Higgs boson h^0 and two heavy Higgs bosons, H^0 and A^0) and two charged (H^+ and H^-). At tree level, the mass of these five Higgs bosons are [42,43]:

$$\begin{aligned} A^0: &\qquad m_{A^0}, \\ h^0: &\qquad m_{h^0} = \tfrac{1}{\sqrt{2}}\left(m_{A^0}^2 + m_Z^2 - \sqrt{(m_{A^0}^2 + m_Z^2)^2 - 4m_{A^0}^2 m_Z^2 \cos^2(2\beta)}\ \right)^{1/2}, \\ H^0: &\qquad m_{H^0} = \tfrac{1}{\sqrt{2}}\left(m_{A^0}^2 + m_Z^2 + \sqrt{(m_{A^0}^2 + m_Z^2)^2 - 4m_{A^0}^2 m_Z^2 \cos^2(2\beta)}\ \right)^{1/2}, \\ H^\pm: &\qquad m_{H^\pm} = \left(m_{A^0}^2 + m_W^2\right)^{1/2}, \end{aligned} \tag{50}$$

where $m_{h^0} < m_{A^0} < m_{H^0}$ at tree level and the mass of A^0 (or the mass of $H^\pm$) is another important Higgs sector parameter of the MSSM. However, according to h^0 expression in Eq.(50), the mass of h^0 is bounded from above:

$$m_{h^0} < m_Z, \tag{51}$$

and, when the mass of A^0 is much larger than the mass of Z boson $m_A^0 \gg m_Z$, called the decoupling limit [44], the tree level mass of h^0 has the form [42]:

$$m_{h^0} = m_Z |\cos(2\beta)|, \tag{52}$$

when we assume the decoupling limit, the light Higgs boson h^0 has a behavior to SM model boson (called SM-like Higgs boson) and the other Higgs bosons A^0, H^0 and $H^\pm$ are mass degenerate as we obtained with `FeynHiggs-2.14.2` in the $m_h^{\text{mod+}}$ scenario, see below.

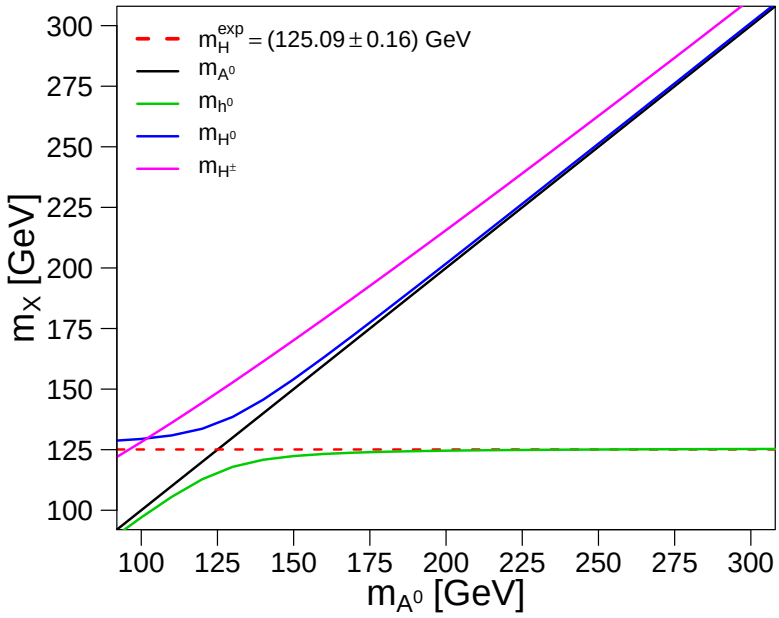

Figure 2: Masses of all MSSM Higgs bosons (h^0, A^0, H^0 and $H^\pm$) as a function of m_{A^0}. In the decoupling limit ($m_{A^0} \gg m_Z$) the light Higgs boson h^0 has a behavior to SM model boson and the other Higgs bosons are mass degenerate. Data obtained with `FeynHiggs-2.14.2` in the $m_h^{\text{mod+}}$ scenario.

According to Eq.(52), the mass of h^0 must be lower than the Z boson mass i.e. m_Z gives an upper limit to the mass of the h^0, $m_{h^0} < m_Z = 91.2$ GeV. This theoretical upper limit for m_{h^0} is far away from the experimental value of $m_H = 125$ GeV at the LHC [9]. However, this difference is corrected by radiative corrections due to contributions from all

sectors of the MSSM [45] then the mass of h^0 has the form

$$m^2_{h^0} = m^{2,\text{tree}}_{h^0} + \Delta m^{2,t/\tilde{t}}_{h^0} + \Delta m^{2,b/\tilde{b}}_{h^0} + \Delta m^{2,\tau/\tilde{\tau}}_{h^0} + \Delta m^{2,\text{QCD}}_{h^0} + ... \tag{53}$$

where $m^{2,\text{tree}}_{h^0}$ is the mass squared of h^0 at tree level, $\Delta m^{2,t/\tilde{t}}_{h^0}$ are one-loop contributions from top-stop sector, $\Delta m^{2,b/\tilde{b}}_{h^0}$ are one-loop contributions from bottom-sbottom sector, $\Delta m^{2,\tau/\tilde{\tau}}_{h^0}$ are one-loop contributions from tau-stau sector and $\Delta m^{2,\text{QCD}}_{h^0}$ are two-loop contributions from QCD corrections [46]. In this work, the most interesting contributions of Eq.(53) are $\Delta m^{2,t/\tilde{t}}_{h^0}$ and $\Delta m^{2,\text{QCD}}_{h^0}$ which are approximately given by [45]

$$\begin{aligned}
\Delta m^{2,t/\tilde{t}}_{h^0} =& \frac{G_F\sqrt{2}}{\pi^2} m_t^4 \left[\log\left(\frac{m_t^2}{M_S^2}\right) \left\{ -\frac{3}{2} - \frac{3}{4}\frac{m_Z^2}{m_t^2}\cos 2\beta - \frac{m_Z^4}{m_t^4}\Lambda\cos^2 2\beta - \right.\right. \\
& \left. - \frac{m_Z^2}{m_{A^0}^2}\cos^2\beta\cos 2\beta \left(6 + \frac{3}{2}\frac{m_Z^2}{m_t^2}(1-4\sin^2\beta) - \frac{m_Z^4}{m_t^4} 8\Lambda\cos 2\beta\sin^2\beta \right) \right\} + \\
& + \left\{ \frac{1}{4}\frac{m_Z^2}{m_t^2} - \frac{11}{80}\frac{m_Z^4}{m_t^4} + \frac{(X_t)^2}{M_S^2}\left(\frac{3}{2} - \frac{1}{2}\frac{m_Z^2}{m_t^2} - \frac{3}{4}\frac{m_t^2}{M_S^2}\right) + \right. \\
& + \frac{(X_t)^4}{M_S^4}\left(-\frac{1}{8} + \frac{1}{2}\frac{m_t^2}{M_S^2} - \frac{3}{8}\frac{m_t^4}{M_S^4}\right) + \frac{(X_t)^6}{M_S^6}\left(-\frac{3}{40}\frac{m_t^2}{M_S^2} + \frac{3}{10}\frac{m_t^4}{M_S^4} - \frac{1}{4}\frac{m_t^6}{M_S^6}\right) + \\
& \left. \left. + \frac{(X_t)^6}{M_S^6}\left(-\frac{3}{56}\frac{m_t^4}{M_S^4} + \frac{3}{14}\frac{m_t^6}{M_S^6} - \frac{3}{16}\frac{m_t^8}{M_S^8}\right) \right\} \left(1 + 4\frac{m_Z^2}{m_{A^0}^2}\cos^2\beta\cos 2\beta\right) \right],
\end{aligned} \tag{54}$$

$$\begin{aligned}
\Delta m^{2,\text{QCD}}_{h^0} =& -\frac{G_F\sqrt{2}}{\pi^2}\frac{\alpha_s}{\pi} m_t^4 \left[4 + 3\log^2\left(\frac{m_t^2}{M_S^2}\right) + 2\log\left(\frac{m_t^2}{M_S^2}\right) - 6\frac{X_t}{M_S} - \right. \\
& - \frac{(X_t)^2}{M_S^2}\left\{ 3\log\left(\frac{m_t^2}{M_S^2}\right) + 8 \right\} + \\
& \left. + \frac{17}{12}\frac{(X_t)^4}{M_S^4} \right] \left(1 + 4\frac{m_Z^2}{m_{A^0}^2}\cos^2\beta\cos 2\beta\right),
\end{aligned} \tag{55}$$

where $X_t = A_t - \mu/\tan\beta$, A_t is the trilinear Higgs-stop coupling and $M_S = \sqrt{m_{\tilde{t}_1} m_{\tilde{t}_2}}$. Λ is given by

$$\Lambda = \frac{1}{8} - \frac{1}{3}\left(1 - \frac{m_W^2}{m_Z^2}\right) + \frac{4}{9}\left(1 - \frac{m_W^2}{m_Z^2}\right)^2. \tag{56}$$

In short, $\Delta m_{h^0}^{2,t/\tilde{t}}$ and $\Delta m_{h^0}^{2,\mathrm{QCD}}$ are proportional to m_t^4 and $\Delta m_{h^0}^{2,b/\tilde{b}}$ and $\Delta m_{h^0}^{2,\tau/\tilde{\tau}}$ are proportional to m_b^4 and m_τ^4, respectively. Now, the upper limit to the mass of the h^0 is $m_{h^0} < 135$ GeV [47] in accordance with the experimental value of $m_H^{\exp}$.

As we can see in [45], in the decoupling limit, when we only consider the corrections due to one-loop contributions for the calculation of m_{h^0}, the positions of extrema for the mass of h^0 are found

$$\frac{A_t - \frac{\mu}{\tan\beta}}{M_S} = \begin{cases} \sqrt{6} & (\text{maximum}) \\ 0 & (\text{minimum}) \\ -\sqrt{6} & (\text{maximum}) \end{cases} . \tag{57}$$

Now, taking into acccount the two-loop contribution $\Delta m_{h^0}^{2,\mathrm{QCD}}$ for the calculation of m_{h^0}, the positions of extrema for the mass of h^0 change in the following way

$$\frac{A_t - \frac{\mu}{\tan\beta}}{M_S} = \begin{cases} \sqrt{6} - \frac{\alpha_s}{\pi}\left[-1 + 3\sqrt{6} - \sqrt{6}\log\left(\frac{m_t^2}{M_S^2}\right)\right] & (\approx +2;\ \text{maximum}) \\ -2\frac{\alpha_s}{\pi} & (\approx 0;\ \text{minimum}) \\ -\sqrt{6} + \frac{\alpha_s}{\pi}\left[+1 + 3\sqrt{6} - \sqrt{6}\log\left(\frac{m_t^2}{M_S^2}\right)\right] & (\approx -2;\ \text{maximum}) \end{cases} , \tag{58}$$

where the maxima are moved to smaller absolute values of $\left(A_t - \frac{\mu}{\tan\beta}\right)/M_S$ and the minimun stays close to zero.

Finally, in the same way as the SM, the Lagrangian of the MSSM has couplings of neutral Higgs bosons with SM fermions [48]:

- Coupling with t quarks (idem to u and c quarks):

$$\mathcal{L}_{\bar{t}t} = -\frac{g_2 m_t}{2m_W}\frac{\cos\alpha}{\sin\beta}\bar{t}t\ h^0 - \frac{g_2 m_t}{2m_W}\frac{\sin\alpha}{\sin\beta}\bar{t}t\ H^0 + \frac{g_2 m_t}{2m_W}\frac{1}{\tan\beta}i\bar{t}\gamma^5 t\ A^0, \tag{59}$$

- Coupling with b quarks (idem to d and s quarks):

$$\mathcal{L}_{\bar{b}b} = +\frac{g_2 m_b}{2m_W}\frac{\sin\alpha}{\cos\beta}\bar{b}b\ h^0 - \frac{g_2 m_b}{2m_W}\frac{\cos\alpha}{\cos\beta}\bar{b}b\ H^0 + \frac{g_2 m_b}{2m_W}\tan\beta i\bar{b}\gamma^5 b\ A^0. \tag{60}$$

- Coupling with τ leptons (idem to e and μ leptons):

$$\mathcal{L}_{\bar{\tau}\tau} = +\frac{g_2 m_\tau}{2m_W}\frac{\sin\alpha}{\cos\beta}\bar{\tau}\tau\ h^0 - \frac{g_2 m_\tau}{2m_W}\frac{\cos\alpha}{\cos\beta}\bar{\tau}\tau\ H^0 + \frac{g_2 m_\tau}{2m_W}\tan\beta i\bar{\tau}\gamma^5\tau\ A^0, \tag{61}$$

where, at tree level, the mixing angle α between m_{A^0} and $\tan\beta$ has the form

$$\tan(2\alpha) = \frac{m_{A^0}^2 + m_Z^2}{m_{A^0}^2 - m_Z^2}\ \tan(2\beta). \tag{62}$$

Notice a very important fact, the Eqs.(59)−(61) have similar form that coupling of SM Higgs boson $H^{\rm SM}$ with fermions (39) but now it is necessary to include "MSSM corrections" of the form of α and β trigonometric functions.

2.3.2 Sfermions: squarks and sleptons

In addition to the quarks and leptons that appear in the SM, the MSSM includes the superpartners of these particles which are known as squarks and sleptons. For each fermionic degree of freedom (f_L, f_R) we have two new sfermionic degree of freedom $(\tilde{f}_L, \tilde{f}_R)$ with spin 0. In order to get physical states [49] it is necessary to build a mass matrix $\mathbf{M}^2_{\tilde{f}}$ that contains mix terms which will mix with the eigenstates $(\tilde{f}_L, \tilde{f}_R)$ as

$$\mathcal{L}_{\text{sfermion mass}} = -\begin{pmatrix}\tilde{f}_L^* & \tilde{f}_R^*\end{pmatrix}\mathbf{M}^2_{\tilde{f}}\begin{pmatrix}\tilde{f}_L \\ \tilde{f}_R\end{pmatrix}, \tag{63}$$

where $\mathbf{M}^2_{\tilde{f}}$ contains, among other contributions, terms from the soft SUSY-breaking parameters that heavily affect the mass of sfermions, being these greater than the mass of fermions. The mass matrix of the stops has the form [50]

$$\mathbf{M}^2_{\tilde{t}} = \begin{pmatrix} m_t^2 + M^2_{\tilde{Q}_3} + D_{\tilde{u}_L} & m_t\,(A_t - \mu/\tan\beta) \\ m_t\,(A_t - \mu/\tan\beta) & m_t^2 + M^2_{\tilde{u}_3} + D_{\tilde{u}_R}\end{pmatrix}, \tag{64}$$

where $M_{\tilde{Q}_3}$ and $M_{\tilde{u}_3}$ are the soft SUSY-breaking mass parameters of the third generation of squarks and u-type squarks, respectively (In Appendix B it introduced $M_{\rm SUSY}$ as $M_{\rm SUSY} = M_{\tilde{Q}_3} = M_{\tilde{u}_3}$). The form of $D_{\tilde{u}_L}$ and $D_{\tilde{u}_R}$ are function of $\tan\beta$, m_Z and another parameters, but these complete expressions are not important for this work. The mass matrix of the sbottoms and staus are built in a similar way, being these matrices [50]:

$$\mathbf{M}^2_{\tilde{b}} = \begin{pmatrix} m_b^2 + M^2_{\tilde{Q}_3} + D_{\tilde{d}_L} & m_b\,(A_b - \mu\tan\beta) \\ m_b\,(A_b - \mu\tan\beta) & m_b^2 + M^2_{\tilde{d}_3} + D_{\tilde{d}_R}\end{pmatrix}, \tag{65}$$

$$\mathbf{M}^2_{\tilde{\tau}} = \begin{pmatrix} m_\tau^2 + M^2_{\tilde{L}_3} + D_{\tilde{e}_L} & m_\tau\,(A_\tau - \mu\tan\beta) \\ m_\tau\,(A_\tau - \mu\tan\beta) & m_\tau^2 + M^2_{\tilde{e}_3} + D_{\tilde{e}_R}\end{pmatrix}, \tag{66}$$

where $M_{\tilde{L}_3}$ and $M_{\tilde{e}_3}$ are the soft SUSY-breaking mass parameters of the third generation of sleptons and $M_{\tilde{d}_3}$ are the soft SUSY-breaking mass parameters of the third generation of d-type squarks. Same for Eq.(64), the complete expresions for $D_{\tilde{d}_L}$, $D_{\tilde{d}_R}$, $D_{\tilde{e}_L}$ and $D_{\tilde{e}_R}$ are not important for this work. Notice that the non-diagonal elements in Eqs.(64)−(66) are proportional to m_t, m_b and m_τ, respectively.

Finally, in order to get physical states it is necessary to diagonalize the mass matrix. For this, it is neccesary to include a rotation matrix $U_{\tilde{f}}$ that mixes the states $(\tilde{f}_L, \tilde{f}_R)$ in order to obtain the physical states $(\tilde{f}_1, \tilde{f}_2)$ i.e. $(\tilde{f}_1, \tilde{f}_2)$ are linear combinations of states $(\tilde{f}_L, \tilde{f}_R)$. For example, the mass eigenstates of physical stops $(\tilde{t}_1, \tilde{t}_2)$ have the form

$$\mathcal{L}_{m_{\tilde{t}}} = - \begin{pmatrix} \tilde{t}_1^* & \tilde{t}_2^* \end{pmatrix} \begin{pmatrix} m^2_{\tilde{t}_1} & 0 \\ 0 & m^2_{\tilde{t}_2} \end{pmatrix} \begin{pmatrix} \tilde{t}_1 \\ \tilde{t}_2 \end{pmatrix} = -m^2_{\tilde{t}_1} \tilde{t}_1^* \tilde{t}_1 - m^2_{\tilde{t}_2} \tilde{t}_2^* \tilde{t}_2. \tag{67}$$

The mix of the states $(\tilde{f}_L, \tilde{f}_R)$ from the rotation matrix $U_{\tilde{f}}$ is obtain as follow

$$\begin{pmatrix} \tilde{t}_1 \\ \tilde{t}_2 \end{pmatrix} = \begin{pmatrix} \cos\theta_{\tilde{t}} & -\sin\theta_{\tilde{t}} \\ \sin\theta_{\tilde{t}} & \cos\theta_{\tilde{t}} \end{pmatrix} \begin{pmatrix} \tilde{t}_L \\ \tilde{t}_R \end{pmatrix}, \tag{68}$$

where $\theta_{\tilde{t}}$ is the stop mixing angle. With an analogous procedure it is possible to developed the mass eigenstates of physical sbottoms $(\tilde{b}_1, \tilde{b}_2)$ and staus $(\tilde{\tau}_1, \tilde{\tau}_2)$.

2.3.3 Gauge bosons and gauginos

In the MSSM, each of the electroweak gauge bosons (B and W^i with $i = 1, 2, 3$) have associated a superpartners with 1/2 spin called gauginos ($\tilde{B}$, $\tilde{W}^{(i)}$ with $i = 1, 2, 3$) [51]. These superpartners are the electroweak gauginos fermions. In this new model, at the same way to SM, the B boson and $W^{(3)}$ will mix to obtain the photon γ and the Z^0 boson and the $W^{(1)}$ and $W^{(2)}$ will mix to form the $W^\pm$ bosons. On the other hand, the gauginos are not physical states. As we will see in the following section, it is necessary that these gauginos mix with Higgsinos in order to give rise to physical states i.e. to give rise physical particles. This particles are called neutralinos and charginos which are discussed in Sec. 2.3.4. Finally, the massless gluon g (the force-carrying particle of the strong interaction) has associated a superpartners with 1/2 spin called gluino $\tilde{g}$ that, unlike the g, it has mass [52].

2.3.4 Neutralinos and charginos

At the similar way to gauge bosons mix among them in order to obtain γ, Z^0 and $W^\pm$, the Higgsinos and gauginos will mix in order to give rise physical particles which are called neutralinos and charginos.

The neutralinos $\tilde{\chi}_i^0$ (with $i = 1, 2, 3, 4$) are the eigenstates formed by the mixture of neutral higgsinos ($\tilde{H}_u^0, \tilde{H}_d^0$) with the neutral gauginos ($\tilde{B}, \tilde{W}^{(3)}$). The mass matrix of neutralinos $\mathbf{M}_{\tilde{N}}$ can be written as [53]

$$\mathbf{M}_{\tilde{N}} = \begin{pmatrix} M_1 & 0 & -m_Z \cos\beta \sin\theta_W & m_Z \sin\beta \sin\theta_W \\ 0 & M_2 & m_Z \cos\beta \cos\theta_W & -m_Z \sin\beta \cos\theta_W \\ -m_Z \cos\beta \sin\theta_W & m_Z \cos\beta \cos\theta_W & 0 & -\mu \\ m_Z \sin\beta \sin\theta_W & -m_Z \sin\beta \cos\theta_W & -\mu & 0 \end{pmatrix}, \tag{69}$$

where M_1 and M_2 are soft SUSY-breaking gauginos masses i.e. the neutralinos masses depends on M_1, M_2 and two Higgs sector parameter (μ and $\tan\beta$). From the diagonalization of $\mathbf{M}_{\tilde{N}}$ the mass of the four neutralinos $m_{\tilde{\chi}_i^0}$ ($i = 1, ..., 4$) with $m_{\tilde{\chi}_1^0} < m_{\tilde{\chi}_2^0} < m_{\tilde{\chi}_3^0} < m_{\tilde{\chi}_4^0}$ are the eigenvalues of Eq.(69). If $M_1 < M_2 < \mu$ then the mass of $\tilde{\chi}_1^0$ and $\tilde{\chi}_2^0$ will depend of M_1 and M_2, respectilvely, and the mass of $\tilde{\chi}_3^0$ and $\tilde{\chi}_4^0$ will depend of $|\mu|$ [54]. From this, it is important to highlight the lightest neutralino $\tilde{\chi}_1^0$ because is an excellent candidate for Dark Matter, as will be discussed in Sec. 2.3.5.

On the other hand, analogously to the neutralinos, the charginos $\tilde{\chi}_i^{\pm}$ (with $i = 1, 2$) are the eigenstates formed by the mixture of charged higgsinos ($\tilde{H}_u^+, \tilde{H}_d^-$) with charged gauginos ($\tilde{W}^+, \tilde{W}^-$). The mass matrix of charginos $\mathbf{M}_{\tilde{C}}$ can be expressed as [53]

$$\mathbf{M}_{\tilde{C}} = \begin{pmatrix} 0 & 0 & M_2 & \sqrt{2}\cos\beta m_W \\ 0 & 0 & \sqrt{2}\sin\beta m_W & \mu \\ M_2 & \sqrt{2}\sin\beta m_W & 0 & 0 \\ \sqrt{2}\cos\beta m_W & \mu & 0 & 0 \end{pmatrix}, \tag{70}$$

where, at the same way to Eq.(69), the charginos masses depend on M_1, M_2, μ and $\tan\beta$. From the diagonalization of $M_{\tilde{C}}$, the mass of the charginos can be written as follows [55]

$$\begin{aligned} m_{\tilde{\chi}_1^{\pm}} &= \frac{1}{\sqrt{2}} \Big(M_2^2 + |\mu|^2 + 2m_W^2 - \\ &\quad - \sqrt{(M_2^2 + |\mu|^2 + 2m_W^2)^2 - 4|m_W^2 \sin 2\beta - |\mu| M_2|^2} \Big)^{1/2}, \\ m_{\tilde{\chi}_2^{\pm}} &= \frac{1}{\sqrt{2}} \Big(M_2^2 + |\mu|^2 + 2m_W^2 + \\ &\quad + \sqrt{(M_2^2 + |\mu|^2 + 2m_W^2)^2 - 4|m_W^2 \sin 2\beta - |\mu| M_2|^2} \Big)^{1/2}, \end{aligned} \tag{71}$$

where $m_{\tilde{\chi}_1^{\pm}} < m_{\tilde{\chi}_2^{\pm}}$ and, unlike the masses of the neutralinos, it does not depend on M_1 parameter.

2.3.5 R-parity

Within the MSSM it is possible to include a new symmetry in order to solve some anomalies of this model [56]. That new symmetry is called R-parity [57] and, in the MSSM, it is assumed to be an exact symmetry. R-parity can be expressed as

$$R = (-1)^{3B+L+2s}, \tag{72}$$

where B and L are the baryon and lepton number, respectively, and s is the spin of the particle [56]. As we be deduced in Eq.(72), all the SM particles have R-parity $+1$ (R-parity even) and their superpartners have R-parity -1 (R-parity odd). Moreover, as it is exposed in [58], it is necessary to show two corollaries:

- In colliders experiment, the supersymmetric particles can only be produced in pairs.
- Heavier supersymmetric particles can decay only into a SM particle and a lighter SUSY particle.

According to these points, the most important consequence of R-parity conservation is that the lightest supersymmetric particle (LSP) must be stable. In the MSSM, the LSP corresponds with the lightest neutralino $\tilde{\chi}_1^0$ [58] which has not electric charge. As we know, the Dark matter must be neutral[9] thus the $\tilde{\chi}_1^0$ is a perfect candidate to Dark matter since this supersymmetric particle is agree with its features because it is stable, neutral and it can has only weak interaction.

2.3.6 Solutions to Standard Model problems

One of the reasons to consider the MSSM as a good candidate to replace the SM is because it solves many of the flaws that this model has. In this section we show the MSSM solutions to the problems mentioned in Sec. 2.1.6.

Candidate for dark matter

As we discussed in Sec. 2.3.5, the lightest neutralino is a perfect candidate to be dark matter because it is stable, neutral and almost does not interact with the matter (only weak interaction) so the search for particles with the neutralinos characteristics at the LHC experiments it is important today [59]. In addition to that, there are SUSY theories that include gravity know as Supergravity (SUGRA) theories [60], where the gravitino, the superpartner of the graviton, can be a candidate to be dark matter.

[9] The Dark matter does not interact with electromagnetic radiation.

Strong-Electroweak unification at 10^{16} GeV

In the MSSM, with SUSY particles at a scale of $\Lambda_{\text{SUSY}} = \mathcal{O}(1)$ TeV, it is possible to get that the gauge couplings g_s, g_1 and g_2 converge to a common value for a energy scale around 10^{16} GeV when their particles contributions are introduced in the running (with energy) of the gauge couplings. For a complete development of this result see [61].

Corrections to the Higgs boson mass

In 2002, the mass of the (light) Higgs boson had been predicted to be between 114 GeV (the lower search bound from LEP) and 135 GeV (the upper limit from the radiative corrections [10]). The experimental value lies might in this interval. As we can see in Sec. 2.3.1, the completeness that the MSSM introduces in the Higgs sector is quite remarkable and it responds very well to these experimental demands. First, because the constribution of the superpartners particles into radiative corrections makes that the mass of the Higgs boson does not diverge until the Planck scale. And, on the other hand, as it is shown in Eqs.(50, 53, 54 and 55), the MSSM provides an analytical expression for the Higgs boson mass (in the SM, it is a free parameter).

2.4 The W boson sector of the MSSM

In this section we will introduce the basic ideas in order to understand the prediction of the mass of W boson within the MSSM m_W^{MSSM} in constrast with the SM prediction m_W^{SM}. This section has the following structure:

- First, it shows an important experimental result which is an useful tool inside the W boson sector at the time to make predictions.
- Then, we show all the contributions (one-loop) that could affect within the calculation of m_W to a greater or lesser extent.
- With that, it is concluded with a comparison between present and future predictions of m_W, both experimental and theoretical.

In experimental physics, a way to determine the W boson mass is from the measurement of the Fermi's constant G_μ which can be obtained from the muon decay rate [62], see Fig. 3. At the current time, the accurate value of G_μ is [19]

$$G_\mu = (1.1663787 \pm 0.0000006) \cdot 10^{-5} \text{ GeV}^{-2}. \tag{73}$$

As will be seen below, to know accurately G_μ is important to predict the mass of the W boson. In addition to that, both in the SM and in the MSSM, G_μ can be written as [63]

$$\frac{G_\mu}{\sqrt{2}} = \frac{e^2}{8\left(1-\frac{m_W^2}{m_Z^2}\right)m_W^2}(1+\Delta r), \tag{74}$$

where Δr is the sum of the all (non-QED) quantum corrections (the QED radiative corrections [64–66] are already included in G_μ) that are obtained from muon decay, see Fig. 3. It is important to highlight that Δr includes all contribution of the particles in loop diagrams which implies that Δr depends on all parameters of the model i.e.

$$\Delta r = \Delta r(m_W, m_Z, m_t, \alpha, \alpha_s, ..., X), \tag{75}$$

where X includes [63]

$$X = \begin{cases} m_{H^{\rm SM}} & \text{(in the SM)} \\ m_{h^0}, m_{A^0}, m_{H^0}, m_{H^\pm}, \tan\beta, A_f, m_{\tilde{f}}, ... & \text{(in the MSSM)} \end{cases}.$$

Then, depending on the set of parameters (and their values) in $\Delta r(..., X)$, according to Eq. (74), it is possible to obtain a theoretical prediction of m_W. So, $m_W^{\rm SM}$ (defined by $\Delta r(..., X^{\rm SM})$, being $X^{\rm SM} = m_{H^{\rm SM}}$) and $m_W^{\rm MSSM}$ (defined by $\Delta r(..., X^{\rm MSSM})$, being $X^{\rm MSSM}$ the free MSSM parameters) are the theoretical predictions of the mass of the W boson in the SM and the MSSM, respectively. Here it should be kept in mind that the SM prediction for the mass of the W boson is $m_W^{\rm SM} = (80.361 \pm 0.004)$ GeV [67] which is below the current experimental value $m_W^{\rm exp} = (80.379 \pm 0.013)$ GeV, see also Tab. 3 (below).

Finally, studying different set of parameters and comparing $m_W^{\rm MSSM} - m_W^{\rm SM}$ with the experimental value $m_W^{\rm exp}$ it is possible to test the MSSM i.e. to delimit the value of the MSSM free parameters.

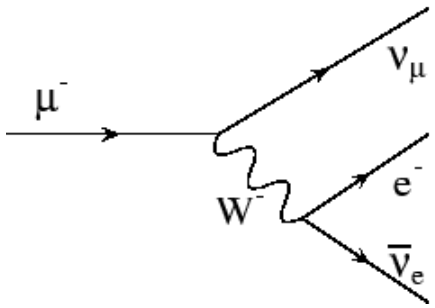

Figure 3: Tree level diagram of muon decay in the SM. It is shown as the W boson is the mediating particle of the interaction [68].

However, evaluate $\Delta r(..., X^{\rm MSSM})$ is not a simple task in the MSSM (From now on, $\Delta r(..., X^{\rm MSSM})$ is expressed as Δr). According to [63], the complet one-loop result for $\Delta r^{(\alpha)}$ has the form

$$\Delta r^{(\alpha)} = \Delta\alpha - \frac{\cos^2\theta_W}{\sin^2\theta_W}\Delta\rho + \Delta r^{(\alpha)}_{\rm rem}, \tag{76}$$

where $\Delta\alpha \propto \log\left(\frac{m_f}{m_Z}\right)$ of all fermions and $\Delta r^{(\alpha)}_{\rm rem} \propto \log\left(\frac{m_{h^0}}{m_W}\right)$. At last, $\Delta\rho \propto m_t^2$ and it also receives sfermions contributions, in particular from the third generation squarks sector. According to the particles involved, it is possible to divide the one-loop constributions to Δr into four classes:

- The SM contributions of quark and lepton loops in the gauge boson self-energies. Its respective Feynman diagram is shown in Fig. 4.
- The SUSY contributions of squark and slepton loops in the gauge boson self-energies. Its respective Feynman diagram is shown in Fig. 5.
- The Higgs and gauge boson sector contributions in the gauge boson self-energies (Fig. 6 and Fig. 7) and contribution of type vertex and box graphs (Fig. 8).
- The SUSY contributions of neutralinos and charginos in the gauge boson self-energies (Fig. 9) and contribution of type vertex and box graphs (Fig. 10).

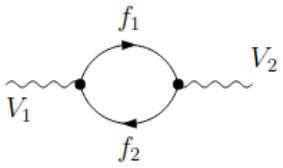

(1)

Figure 4: One loop diagram of lepton and quark contributions to $\Delta r^{(\alpha)}$ via gauge boson self-energies. The $V_1, V_2 = \gamma, W^{\pm}, Z^0$ and $f_1, f_2 = \nu, l, u, d$.

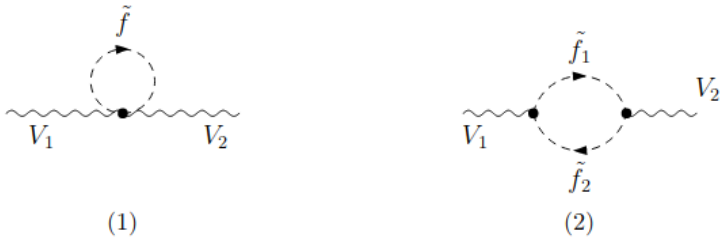

Figure 5: One loop diagram of slepton and squark contributions to $\Delta r^{(\alpha)}$ via gauge boson self-energies. The $V_1, V_2 = \gamma, W^{\pm}, Z^0$ and $\tilde{f}, \tilde{f}_1, \tilde{f}_2 = \tilde{\nu}, \tilde{l}, \tilde{u}, \tilde{d}$.

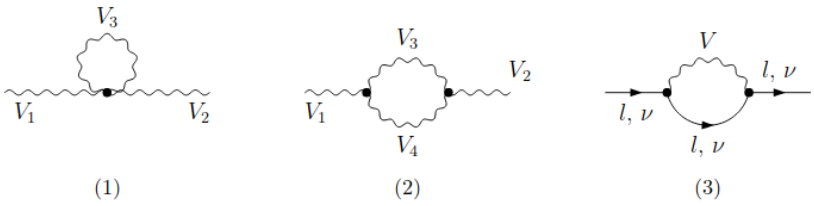

Figure 6: One loop diagram of gauge boson contributions to $\Delta r^{(\alpha)}$ via gauge boson and fermion self-energies. The $V_1, V_2, V_3 = \gamma, W^{\pm}, Z^0$ and the labels l and ν corresponds with electron and muon and the corresponding neutrinos.

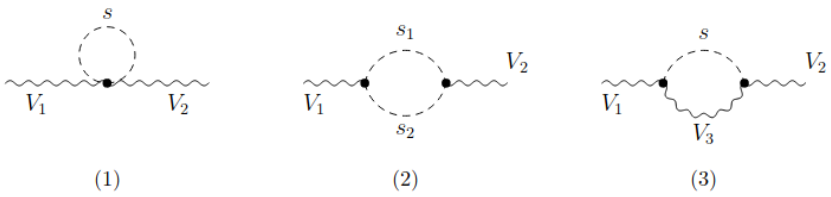

Figure 7: One loop diagram of MSSM Higgs bosons and Goldstone bosons contributions to $\Delta r^{(\alpha)}$ via gauge boson self-energies. The $s, s_1, s_2 = h^0, H^0, A^0, H^{\pm}, G^0, G^{\pm}$.

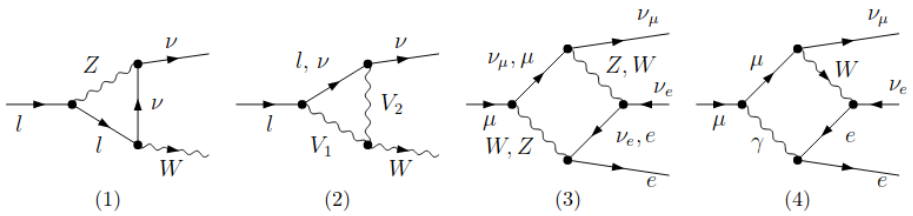

Figure 8: Gauge boson contributions to $\Delta r^{(\alpha)}$ via one-loop vertex and box diagrams. The $V_1, V_2 = \gamma, W^{\pm}, Z^0$ and the labels l and ν corresponds with electron and muon and the corresponding neutrinos.

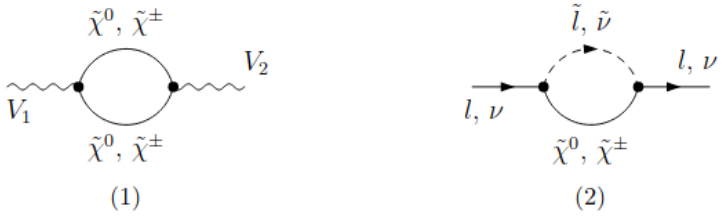

Figure 9: One loop diagram of neutralino/chargino contributions to $\Delta r^{(\alpha)}$ via gauge boson (1) and fermion self-energies (2). The $V_1, V_2 = \gamma, W^{\pm}, Z^0$ and the labels l and ν corresponds with electron and muon and the corresponding neutrinos; the labels $\tilde{l}$ and $\tilde{\nu}$ corresponds with their respective superpartners.

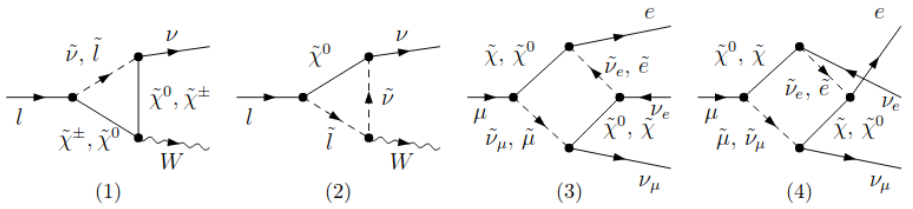

Figure 10: Neutralino and chargino contributions to $\Delta r^{(\alpha)}$ via one-loop vertex and box diagrams. The $V_1, V_2 = \gamma, W^{\pm}, Z^0$ and the labels l and ν corresponds with electron and muon and the corresponding neutrinos; the labels $\tilde{l}$ and $\tilde{\nu}$ corresponds with their respective superpartners.

The form and diagrams for higher-order contributions are more complicated and their expressions are not interesting for this work. For additional information, see [63].

However, in this work it is important to have an estimate of the precision of the theoretical predictions for $m_W^{\rm SM}$ and $m_W^{\rm MSSM}$ in order to find relevant deviations between both predictions. In Tab. 3 we show the theoretical and experimental uncertainties for the mass of the W boson at the current time and those expected values at the future.

Time	$\delta m_W^{\rm exp}$ / MeV	$\delta m_W^{\rm SM}$ / MeV	$\delta m_W^{\rm MSSM}$ / MeV	$\delta m_W^{\rm total}$ / MeV
Present	13	4	$5-9$	$18-22$
Future	3	1	$2-4$	$5-7$

Table 3: Theoretical and experimental uncertainties of the mass of the W boson at the current and future time. The value of $\delta m_W^{\rm total}$ is a combination of experimental and theoretical uncertainty. The present and future experimental uncertainties have been obtained from [11], [69], respectively. The present and future theoretical uncertainties have been obtained from [70], [71] for the SM and from [72], [73] and [63] for the MSSM, respectively. In the MSSM, the uncertainties $\delta m_W^{\rm MSSM}$ decrease for increasing $M_{\rm SUSY}$ and vice versa.

The future accuracy of 3 MeV is expected from a fit to the measurement of the production cross section of $e^+e^- \to W^+W^-$ at the Internacional Linear Collider (ILC). The ILC would be a great tool to study the electroweak and the Higgs sectors, allowing us to check models beyond the SM [74].

Finally, it is important to highlight that the theory uncertainty is caused by the missing high-order corrections in the calculation of $\Delta r(..., X)$.

3 Benchmark Scenarios

In Sec. 2.3, we have introduced the MSSM which is a candidate to extended the SM because it solves many problems that this theory has. However, in favor of SM that has 19 parameters, the MSSM has more than 100 parameters which have to be chosen by hand [10]. This complicates to make any phenomenological analysis. One way to circumvent this problem is to give values to these parameters in so-called benchmark scenarios. The parameters are fixed according to experimental evidences and should exemplify interesting aspects of the MSSM phenomenology.

3.1 The $m_h^{\text{mod+}}$ scenario

In this work, we consider the $m_h^{\text{mod+}}$ scenario [76] which is in agreement with the discovery of Higgs boson at the LHC. Before to expose the paremeter settings used for this scenario, it is necessary to make some modifications of "traditional" set of $m_h^{\text{mod+}}$ parameters:

- Initially, m_{A^0} and $\tan\beta$ were free parameters. However, after the discovery of Higgs boson at the LHC, only a small region in the $m_{A^0} - \tan\beta$ plane (For large m_{A^0} values and low $\tan\beta$ [76]) is in agreement with this discovery. In this work, we fix the value of $\tan\beta$ and $m_{H^\pm}$ (since, when we work with complex parameters, the eigenstates corresponding with h^0, H^0 and A^0 are mixed among them.) according to direct searches at the LHC [77].
- The X_t parameter is changed in order to get that m_{h^0} is inside the range of the measured value of Higgs boson discovered at the LHC. In this work, inside the range $m_{h^0} = (125 \pm 3)$ GeV due to numerical uncertainty.
- From direct searches for SUSY particles at the LCH [78] an increase of the gluino mass is necessary. The low bound is $m_{\tilde{g}} \geq 800$ GeV.

Based on the previous points, the paremeter settings for the $m_h^{\text{mod+}}$ are:

[10] With an understanding of the mechanism that breaks SUSY, the numbers of additional free parameters can likely be drastically reduced. As an example, the "constrained MSSM" (CMSSM) [75] is described by four new free parameters.

m_t	μ	$\tan\beta$	$m_{H^\pm}$	M_1	M_2	M_3	$M_{\tilde{Q}_i,\tilde{u}_i}$	$M_{\tilde{d}_i}$	$M_{\tilde{L}_i,\tilde{e}_i}$	A_t	A_b	A_τ
174.3	200	10	1005	100	200	1500	1500	1000	1000	2000	1500	1500

Table 4: The $m_h^{\text{mod+}}$ scenario input parameters used for the numerical analysis. The couplings A_u and A_c are equal to A_t, A_d and A_s are equal to A_b, A_e and A_μ are equal to A_τ. Except for $\tan\beta$ (dimensionless), the units for all input parameters are given in GeV.

We fix $m_{H^\pm}$ and $\tan\beta$ in our benchmark set-up. Later we will vary the relevant parameters with respect to the ones in Tab. 4. Notice the top quark mass m_t is an input fixed parameter. The value of m_t is somewhat outdated. However, using the current value, which is about 1 GeV lower, would not change the results of this work in a relevant way.

3.2 The `FeynHiggs` code

As seen in the Sec. 2.3.1, the Higgs sector of the MSSM allows us to perform precise theoretical predictions of the properties of the Higgs boson as measured by CMS and ATLAS. This experimental discovery is a good tool to analyze the space of free parameters of this model [79]. However, it is necessary to take into account some considerations.

On the one hand, at tree level, the Higgs sector depends on SM parameters plus two additional MSSM parameters. Moreover, when radiative corrections are introduced the number of free parameters is increased. All of this complicates the calculations. On the other hand, the MSSM contains a spread spectrum of particles: all SM models particles plus five Higgs boson and their respective superpartners. In addition to this, we have already seen that some particles, for example the h^0, have important quantum corrections and others, for example the neutralinos, they are the mixture of the eigenstates of the neutral higgsinos and gauginos. All of the above (and more), to get precise measurements in the MSSM requires a considerable computational capacity.

One such program that can perform these calculations is `FeynHiggs` [10, 46, 49, 79–83] which is a Fortran code that gives numerical predictions for the MSSM Higgs boson phenomenology (such as masses, mixing angles, decay widths, ...). The most remarkable feature of this program is that combines the calculation of the masses of the Higgs bosons using the Feynmann-diagrammatic up to two-loop contributions $\mathcal{O}(\alpha_t\alpha_s, \alpha_b\alpha_s, \alpha_t^2, \alpha_t\alpha_b, \alpha_b^2)$ with a resummation of large logarithmic contributions to all orders. For a more detailed analysis see [79].

These features do `FeynHiggs` to be the first "hybrid code" that uses a combination of both types of calculation. In this work we will use `FeynHiggs-2.14.2` in order to study the dependence of the mass of h^0 with the free parameters of the MSSM. Based on the feautres previously exposed, the numerical uncertainty on the mass of the h^0 is approximately 3 GeV. So, we will consider correct our predictions if they are within the allowed region $m_{h^0} = (125 \pm 3)$ GeV. Also the predictions of m_W^{SM} and m_W^{MSSM} are obtained with `FeynHiggs`. The m_W^{MSSM} calculation is based on [67], the m_W^{SM} calculation on [70].

4 Scanning the space of the MSSM parameters

As we discussed in Sec. 3.1, we consider the $m_h^{\text{mod+}}$ scenario where we assume the decoupling limit [44] ($m_{H^\pm} = 1005$ GeV $\simeq m_{A^0} \gg m_Z$) in which the light Higgs boson h^0 has a similar behavior to SM Higgs boson H^{SM}. Moreover, in this situation, the other Higgs bosons A^0, H^0 and $H^\pm$ are degenerate i.e. $m_{A^0} \approx m_{H^0} \approx m_{H^\pm}$ and their couplings to the rest of particles is nearly similar.

Now we shall be interested in obtaining the mass of h^0 around 125 GeV and, in the allowed parameter space, predict the mass of W boson. For it we use `FeynHiggs-2.14.2`. Additionally we consider the following restrictions based on experimental results:

- The charginos $\tilde{\chi}_i^\pm$ ($i = 1, 2$) mass always greater than 100 GeV [19]. So the lower limit we consider is $m_{\tilde{\chi}_i^\pm} \geq 100$ GeV.
- The stops $\tilde{t}_i$ ($i = 1, 2$) mass always greater than 500 GeV [84]. So the lower limit we consider is $m_{\tilde{t}_i} \geq 500$ GeV.
- The sbottoms $\tilde{b}_i$ ($i = 1, 2$) mass always greater than 500 GeV [85]. So the lower limit we consider is $m_{\tilde{b}_i} \geq 500$ GeV.
- The charged sleptons $\tilde{e}_i$, $\tilde{\mu}_i$ and $\tilde{\tau}_i$ ($i = 1, 2$) mass always greater than 100 GeV [86]. So the lower limit we consider is $m_{\tilde{e},\tilde{\mu},\tilde{\tau}_i} \geq 100$ GeV.
- The neutral sleptons $\tilde{\nu}_e$, $\tilde{\nu}_\mu$ and $\tilde{\nu}_\tau$ mass always greater than 100 GeV [86]. So the lower limit we consider is $m_{\tilde{\nu}_{e,\mu,\tau}} \geq 100$ GeV.

These limits are only approximations to the current exclusion bounds. However, a detailed treatment, involving specialized recasting tools, is beyond the scope of this work. In addition to that, as we mentioned in Sec. 3.2, due to the precision of the code, the mass of h^0 should be always between 122 GeV and 128 GeV. So the m_{h^0} range we consider is $m_{h^0} = (125 \pm 3)$ GeV.

In the following subsections we analyze the dependence of the mass of h^0 with the free parameters of the MSSM. First, we fixed our scenario and then we will vary the free parameters in order to study their dependence with m_{h^0}. In some cases the variation of m_{h^0} will be studied as a function one parameter but, in other cases, we will study the variation of m_{h^0} in a plane of these parameters. For all the cases analyzed, the rest of the MSSM parameters are fixed to the values in Tab. 4. Finally, in the allowed region for the mass of h^0, in Sec. 5 we analyze the dependence of the mass of W boson in the MSSM m_W^{MSSM} with the two-fold purpose:

1. To find the parameters that m_W^{MSSM} is most sensitive to.

2. To constrain the MSSM parameters space via the prediction of m_W^{MSSM}.

4.1 Dependence of m_{h^0} on the sfermions coupling

In this section we study how the mass of h^0 changes as a function of trilinear Higgs-sfermions coupling A_f. However, we only study the contribution of the third generation of sfermions (because we expect that the most important contribution on the mass of h^0 come to the heaviest generation) and, in addition, we are only interested to the trilinear Higgs-stops coupling A_t since the others third generation of sfermions contribution, A_τ and A_b, is negligible (it is shown in Appendix A).

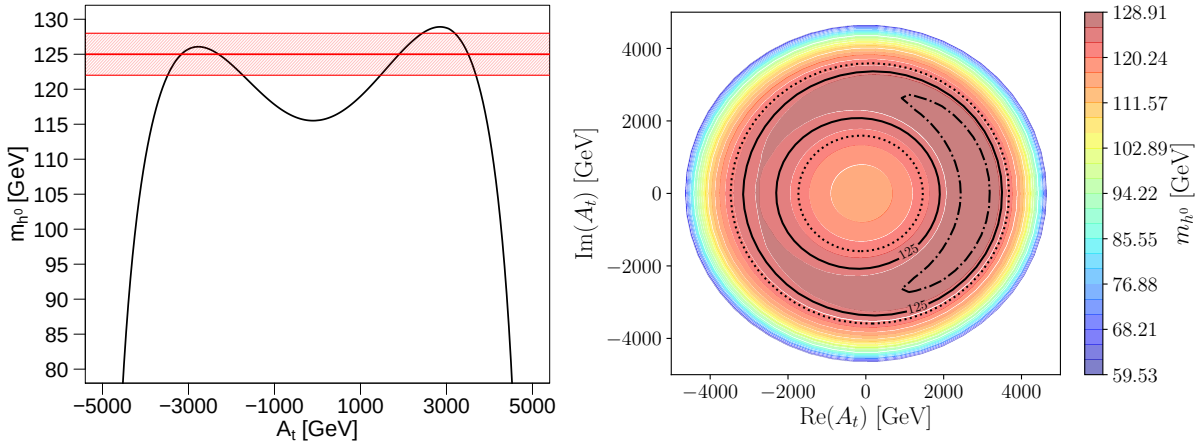

Figure 11: Dependence of m_{h^0} with A_t (left) and in the complex A_t plane (right). The red area (left) denotes the allowed region where $m_{h^0} = (125 \pm 3)$ GeV due to the numerical uncertainty. The solid black line (right) denotes the value of $m_{h^0} = 125$ GeV and the dotted and dash-dotted lines denote the values of $m_{h^0} = 122$ GeV and $m_{h^0} = 128$ GeV, respectively. The rest of the MSSM parameters are set to the values in the $m_h^{\text{mod+}}$ scenario (Tab. 4).

In Fig. 11 it is shown the variation of the mass of h^0 by a change on the A_t where it exists a strong dependence between the m_{h^0} and A_t. On the one hand, it can be seen in the left plot

that the function presents a local minimum around $A_t \simeq 0$ (called minimal stop mixing region) and two maxima (called maximal stop mixing region) around $A_t \simeq -3000$ GeV, with $m_{h^0} \simeq 126$ GeV, and $A_t \simeq 3000$ GeV, with $m_{h^0} \simeq 129$ GeV i.e. approximately inside the allowed region. According to Eq.(57), the function of m_{h^0} presents two maxima for $\left|A_t - \frac{\mu}{\tan\beta}\right| \simeq \sqrt{6} M_S$ when it is not considered two-loop corrections and $\left|A_t - \frac{\mu}{\tan\beta}\right| \simeq 2M_S$ when these are considered as we can see in Eq.(58). In our scenario, $M_S \simeq 1500$ GeV and the predict maximum values is located in $A_t \simeq 2M_S + \frac{\mu}{\tan\beta} \simeq \pm 3000$ GeV in accordance with Eq.(58). Moreover, for large values of $|A_t|$, the mass of h^0 decreases quickly because the contribution of A_t is high but negative, i.e. the contribution of stops sector tends to decrease m_{h^0} for large A_t. It is important to say that it is not possible put a very high A_t value because the mass squared of the light stop becomes negative. On the other hand, in the right plot we can also see that Φ_{A_t} affects the mass of h^0 but it is important to highlight that m_{h^0} largest for A_t in the real line. In view of the foregoing, the coupling A_t is an important paramenter in order to study the mass of h^0. A more detailed discussion will be give in Sec. 4.3.

4.2 Dependence of m_{h^0} on the squarks soft SUSY-breaking mass parameters

In this section we study how the mass of h^0 evolves as a function the squarks soft SUSY-breaking mass parameters $M_{\tilde{X}_3}$ (with $\tilde{X} = \tilde{Q}, \tilde{u}, \tilde{d}$) which are fundamental to determine the masses of the squarks as can be seen in the squarks mass matrices given in Eqs.(64) and (65). Like the previous section, we only study the contribution of third generation of squarks.

In Fig. 12 we show the variation of the mass of h^0 with the soft SUSY-breaking mass parameters of the squarks i.e. the dependence of m_{h^0} with $M_{\tilde{Q}_3}$, $M_{\tilde{u}_3}$ and $M_{\tilde{d}_3}$ for different A_t values. In all plots in Fig. 12 it can be seen that exists a strong influence of $M_{\tilde{Q}_3}$ and $M_{\tilde{u}_3}$ with m_{h^0} because, according to Eq.(64), these soft SUSY-breaking parameters directly affect the mass of the stops so that directly affect the stops sector and, as seen in Sec. 4.1, this sector is the most important contribution to m_{h^0}. Moreover, we can appreciate that both functions for $M_{\tilde{Q}_3}$ and $M_{\tilde{u}_3}$ present a similar shape: the mass of h^0 increases with the value of $M_{\tilde{Q}_3}$ (or $M_{\tilde{u}_3}$) to a maximum value of m_{h^0} where this maximum is similar for each free parameter $M_{\tilde{Q}_3}$, $M_{\tilde{u}_3}$ and $M_{\tilde{d}_3}$ in each of the analyzed cases. After this maximum value, for large $M_{\tilde{Q}_3}$ and $M_{\tilde{u}_3}$ the mass of h^0 decreases due to the negative contribution of the stops masses because they are located in the denominator to Eq.(54). This decrease in the mass of h^0 is not so abrupt due to logarithmic contributions in Eq.(54). On the other hand, for $A_t = 1500$ GeV (the top left plot in Fig. 12) it can be seen that the behaviour

of $M_{\tilde{Q}_3}$ and $M_{\tilde{u}_3}$ is not similar to $A_t = 2000$ GeV and $A_t = 2500$ GeV. The reason for this numerical behavior stems from the resummed logarithmic contributions, see [87].

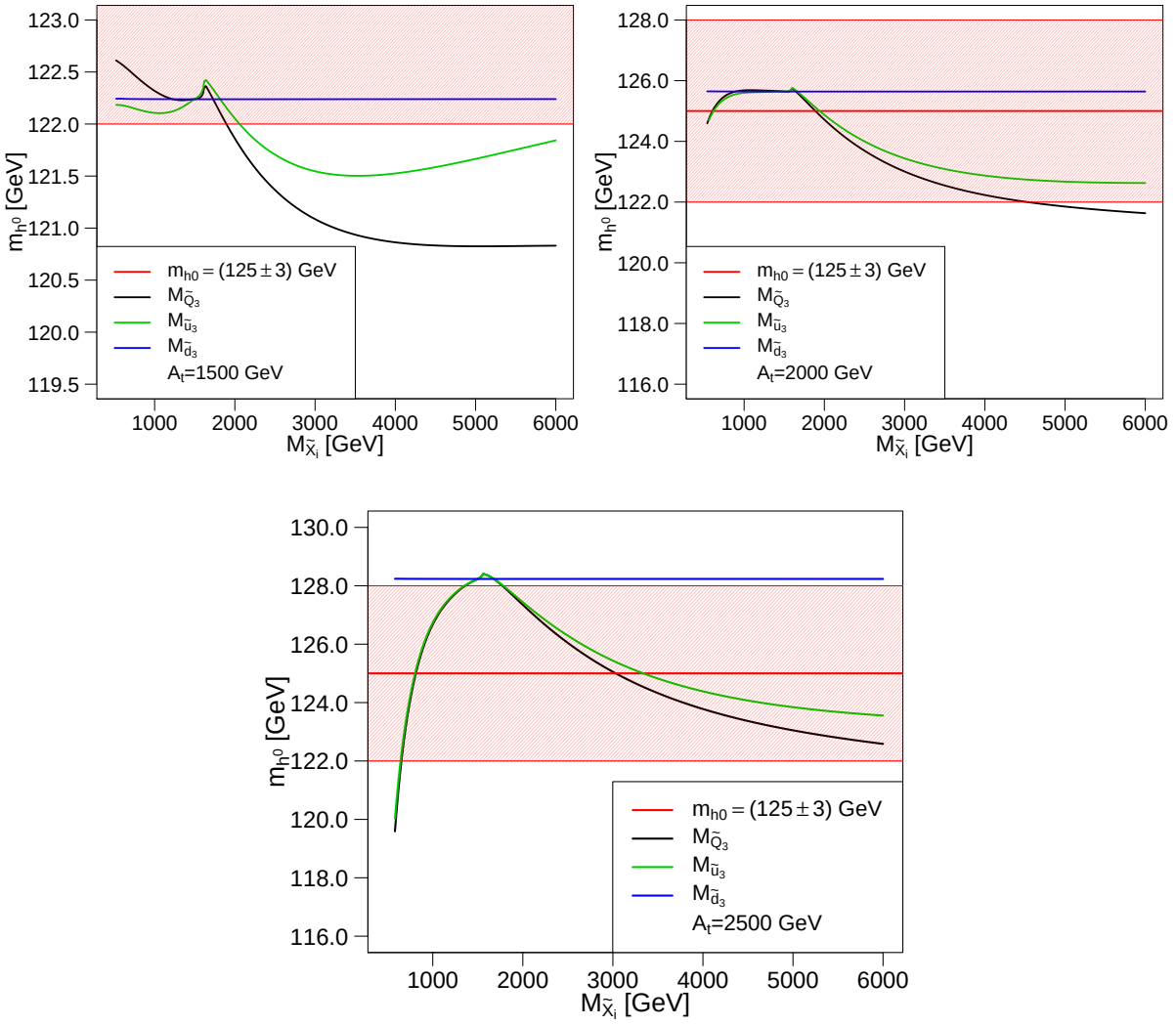

Figure 12: Dependence of m_{h^0} with the squarks soft SUSY-breaking mass parameters with $A_t = 1500$ GeV (top left), $A_t = 2000$ GeV (top right) and $A_t = 2500$ GeV (bottom). The red area denotes the allowed region where $m_{h^0} = (125 \pm 3)$ GeV due to the numerical uncertainty. The rest of the MSSM parameters are set to the values in the $m_h^{\text{mod+}}$ scenario (Tab. 4).

Finally, in all plots in Fig. 12 the dependence with $M_{\tilde{d}_3}$ is very small since its variation does not change the mass of h^0. The soft SUSY-breaking mass parameter $M_{\tilde{d}_3}$, according to Eq.(65), affects the sbottoms sector and, as seen in Appendix A, the contribution of this sector to m_{h^0} is practically negligible.

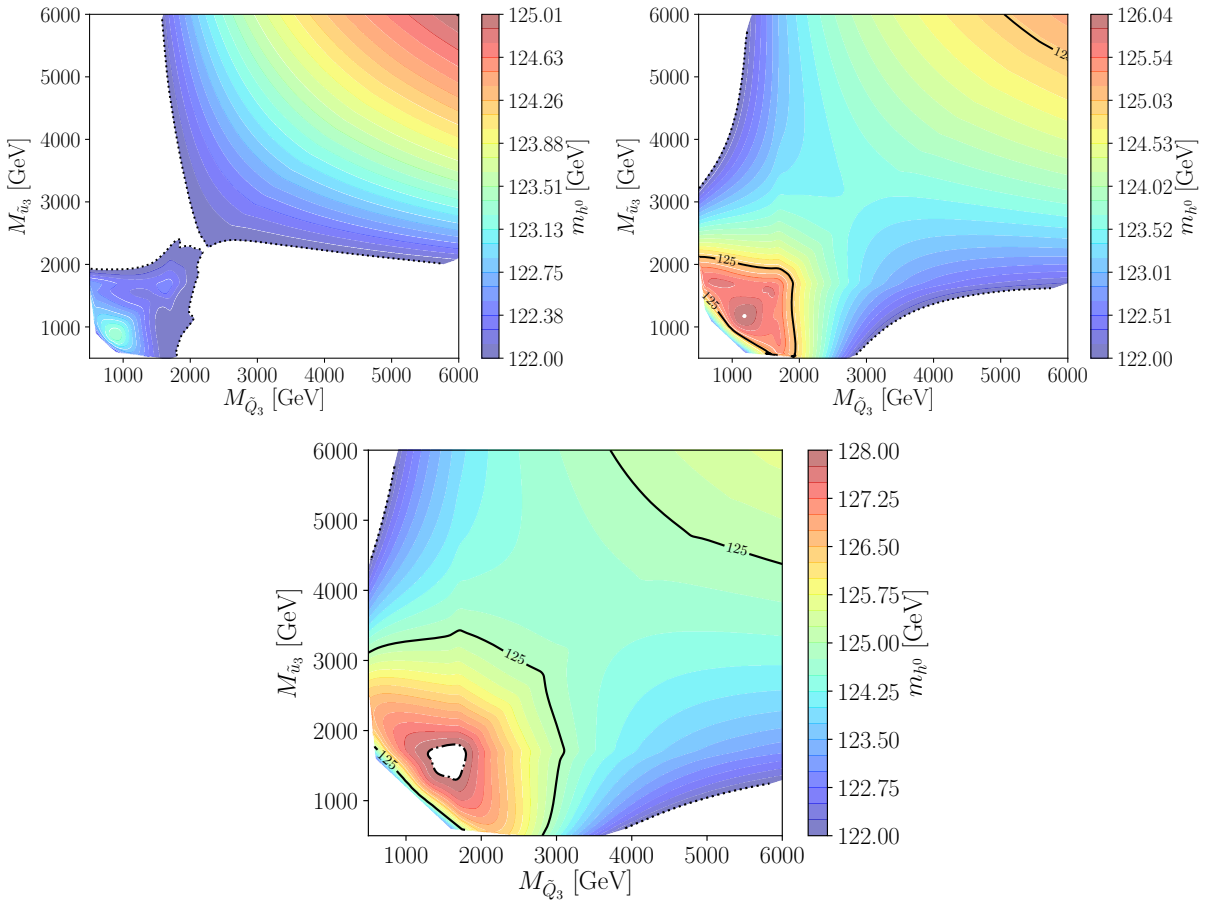

Figure 13: Dependence of m_{h^0} with the plane $M_{\tilde{Q}_3} - M_{\tilde{u}_3}$ for $A_t = 1500$ GeV (left), $A_t = 2000$ GeV (right) and $A_t = 2500$ GeV (bottom). The solid black line denotes the value of $m_{h^0} = 125$ GeV and the dotted and dash-dotted lines denote the values of $m_{h^0} = 122$ GeV and $m_{h^0} = 128$ GeV, respectively. The rest of the MSSM parameters are set to the values in the $m_h^{\text{mod+}}$ scenario (Tab. 4).

In the Fig. 13 is represented the variation of m_{h^0} with the plane $M_{\tilde{Q}_3} - M_{\tilde{u}_3}$ for differents A_t values. It can be seen that the mass of the h^0 strongly changes with the influence of the plane $M_{\tilde{Q}_3} - M_{\tilde{u}_3}$ as we had observed in Fig. 12. But now, this representation allows us to see that m_{h^0} symmetrically evolves with respect to the line $M_{\tilde{Q}_3} = M_{\tilde{u}_3}$. Moreover, it can be seen that the mass of h^0 achieves a maximum when $M_{\tilde{Q}_3} + M_{\tilde{u}_3} \simeq 12000$ GeV for $A_t = 1500$ GeV (nearly outside the limits imposed for this parameters by us) and for the other cases $M_{\tilde{Q}_3} + M_{\tilde{u}_3} \simeq 2400$ GeV for $A_t = 2000$ GeV and $M_{\tilde{Q}_3} + M_{\tilde{u}_3} \simeq 3000$ GeV for $A_t = 2500$ GeV. However, in the cases of $A_t = 1500$ GeV and $A_t = 2500$ GeV (at the left and bottom of Fig. 13, respectively) it can be highlighted the following: in the first case we can see two allowed regions separated by a forbidden region in $M_{\tilde{Q}_3} = M_{\tilde{u}_3} \simeq 2300$ GeV where the m_{h^0} is below 122 GeV. For the second case, it exists a small forbbiden region inside all the allowed values of the plane $M_{\tilde{Q}_3} - M_{\tilde{u}_3}$. This forbbiden region is found in $M_{\tilde{Q}_3} = M_{\tilde{u}_3} \simeq 1800$ GeV where the m_{h^0} is above 128 GeV.

4.3 Dependence of m_{h^0} on the squarks soft SUSY-breaking mass parameters in the complex A_t plane

As seen in the Sec. 4.1 and Sec. 4.2, the most important constributions for the mass of h^0 come from the trilinear Higgs-stops coupling A_t and the squarks soft SUSY-breaking mass parameters $M_{\tilde{Q}_3}$ and $M_{\tilde{u}_3}$. Based on that, in this section we study how the mass of h^0 evolves as a function the complex plane of A_t for different values of $M_{\tilde{Q}_3}$ and $M_{\tilde{u}_3}$ but with the requeriment that $M_{\tilde{Q}_3} = M_{\tilde{u}_3}$.

In Fig. 14 we show the dependence of the mass of h^0 with the complex A_t plane for different values of $M_{\tilde{Q}_3}$ and $M_{\tilde{u}_3}$. First, as we expected for all plots, it can be seen that m_{h^0} is found largest in the real line of A_t and, in addition to that, the maximum value of m_{h^0} increases when the value of $M_{\tilde{Q}_3}$ and $M_{\tilde{u}_3}$ are larger. Moreover, three forbidden regions can be appreciated in all of them but with some of differences that are going to be analyzed below. On the one hand, the first forbidden region (central region with $m_{h^0} < 122$ GeV) at the bottom of Fig. 14 it is found for A_t values lower than 1500 GeV and greater than -1500 GeV for $\Phi_{A_t} \in [0, 2\pi]$. The second forbidden region (internal region with $m_{h^0} > 128$ GeV) is found in 3000 GeV $< A_t <$ 5500 GeV whose width decreases while we go through the complex plane up the negative values of the A_t in real line, whose width is around 1000 GeV. The third forbidden region (external region with $m_{h^0} < 122$ GeV) is found for A_t values greater than 6000 GeV and lower than -5800 GeV for $\Phi_{A_t} \in [0, 2\pi]$.

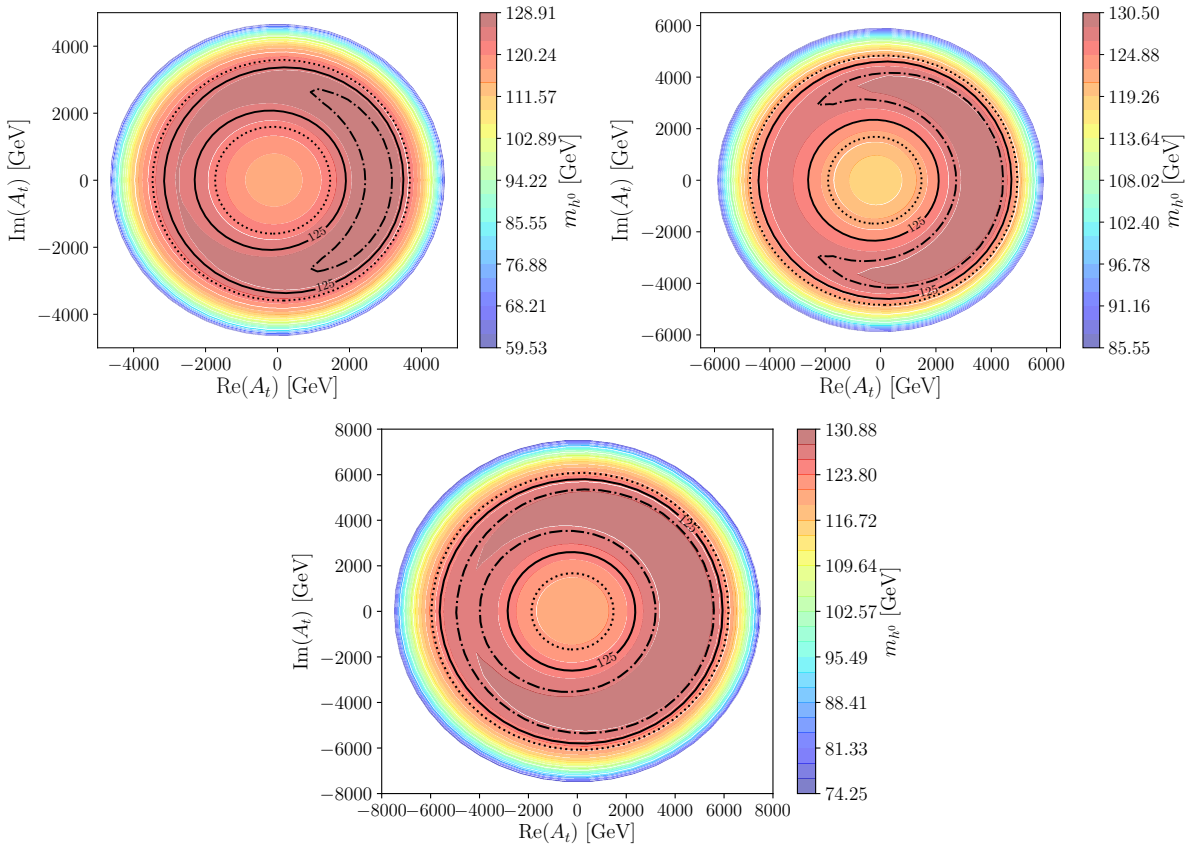

Figure 14: Dependence of m_{h^0} in the complex A_t with $M_{\tilde{Q}_3} = M_{\tilde{u}_3} = 1500$ GeV (left), $M_{\tilde{Q}_3} = M_{\tilde{u}_3} = 2000$ GeV (right) and $M_{\tilde{Q}_3} = M_{\tilde{u}_3} = 2500$ GeV (bottom). The solid black line denotes the value of $m_{h^0} = 125$ GeV and the dotted and dash-dotted lines denote the values of $m_{h^0} = 122$ GeV and $m_{h^0} = 128$ GeV, respectively. The rest of the MSSM parameters are set to the values in the $m_h^{\text{mod+}}$ scenario (Tab. 4).

On the other hand, in the other plots in Fig. 14 the external forbidden region begins at smaller values of A_t i.e. it is more restrictive. For $M_{\tilde{Q}_3} = M_{\tilde{u}_3} = 1500$ GeV (at the left of Fig. 14) it is found in $A_t > 3500$ GeV and $A_t < -3000$ GeV and, at the right of Fig. 14, that external forbidden region is found in $A_t > 5000$ GeV and $A_t < -4000$ GeV for $\Phi_{A_t} \in [0, 2\pi]$ in both plots. Moreover, the internal forbidden region is smaller than the case of $M_{\tilde{Q}_3} = M_{\tilde{u}_3} = 2500$ GeV (in the ranges 2500 GeV $\leq \mathrm{A_t} \leq$ 3000 GeV and 3000 GeV $\leq \mathrm{A_t} \leq$ 4500 GeV for the first and second case, respectively) and only it is found for positive A_t values with $\Phi_{A_t} \in \left[\frac{3\pi}{2}, \frac{\pi}{2}\right]$. The size of the central region is similar

to $A_t = 2500$ GeV in both cases. All the rest of A_t complex plane is in accordance with the prediction of the mass of h^0 i.e. it is within the range of phenomenological validity for our predictions.

4.4 Dependence of m_{h^0} on the sleptons soft SUSY-breaking mass parameters

In this section we study how the mass of h^0 evolves as a function the sleptons soft SUSY-breaking mass parameters $M_{\tilde{X}_3}$ (with $\tilde{X} = \tilde{L}, \tilde{e}$) which are fundamental to determine the masses of the sleptons as can be seen in the sleptons mass matrix given in Eq.(66). Like the previous section, we only study the contribution of third generation of sleptons.

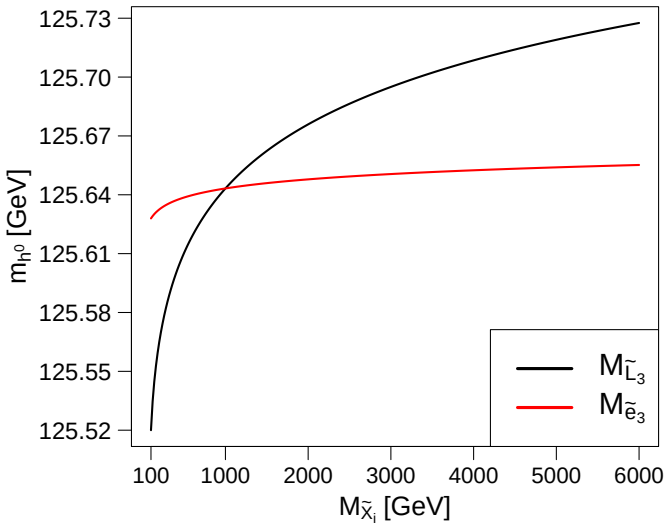

Figure 15: Dependence of m_{h^0} with the sleptons soft SUSY-breaking mass. The rest of the MSSM parameters are set to the values in the $m_h^{\text{mod+}}$ scenario (Tab. 4).

In Fig. 15 we show the dependence of m_{h^0} with the soft SUSY-breaking mass of sleptons i.e. $M_{\tilde{L}_3}$ and $M_{\tilde{e}_3}$. We can see a small influence of $M_{\tilde{L}_3}$ and $M_{\tilde{e}_3}$ with the mass of h^0 since, as we shown in Eq.(66), these soft SUSY-breaking mass parameters of the slepton sector only affect the mass of the staus and, it is shown in Appendix A, his contribution is practically negligible compared to the contribution of the stops. Thus, any slepton contribution is not so important as the stop contribution for the mass of h^0.

5 Numerical analysis of $m_W^{\rm MSSM}$

In Sec. 4 we have scanned the space of the MSSM parameters in order to analyze the dependence of m_{h^0} with the free MSSM parameters and, with that, to find ranges of these paramaters that are in agreement with $m_{h^0} = (125 \pm 3)$ GeV. Now, in these allowed regions, we will study how affect these MSSM parameters the prediction of the W boson mass $m_W^{\rm MSSM}$, i.e. how much the MSSM prediction of the W boson mass differs from the SM prediction $m_W^{\rm SM}$. Based on these results and the data indicated in Tab. 3, we will indicate implications for the values of the MSSM free parameters.

5.1 Dependence of $m_W^{\rm MSSM}$ on the stop coupling

In this section we study how the triliear Higgs-stop coupling A_t affects the mass of W boson $m_W^{\rm MSSM}$ and how much does it differs from the SM prediction $m_W^{\rm SM}$.

In Fig. 16 it is shown the variation of $m_W^{\rm MSSM}$ as a function of A_t. On the one hand, in the left plot of Fig. 16 we can identify three regions where the mass of h^0 are not excluded by our numerical uncertainty indicated by the white stripes. In addition to that, the red area denotes the W boson mass uncertainty at the current time $m_W^{\rm exp,today} = (80.379 \pm 0.018)$ GeV and the green area denotes the future uncertainty of the W boson mass $m_W^{\rm exp,future} = (80.379 \pm 0.005)$ GeV. The first allowed region are found between $A_t = -3500$ GeV and $A_t = -1700$ GeV where $m_W^{\rm MSSM}$ changes a maximum of 7 MeV. The second allowed region are found between $A_t = 1450$ GeV and $A_t = 2450$ GeV where $m_W^{\rm MSSM}$ changes a maximum of 2 MeV. For both regions, these effects are too small for today's precision in $m_W^{\rm MSSM}$. Also with a future resolution of 5 MeV we can hardly see an remarkable effect. However, the last allowed region are found between $A_t = 3115$ GeV and $A_t = 3700$ GeV where $m_W^{\rm MSSM}$ changes a maximum of 8 MeV. Within this region, these effects are large enough in order to detect an important change of $m_W^{\rm MSSM}$ because of the SUSY-breaking parameters with the future's precision.

On the other hand, at the right of the Fig. 16 it is shown the difference between the MSSM and the SM predictions of the W boson mass in the complex plane of A_t. As in Sec. 4, the solid black line denotes the value of $m_{h^0} = 125$ GeV and the dotted and dash-dotted lines denote the values of $m_{h^0} = 122$ GeV and $m_{h^0} = 128$ GeV, respectively. First, we can see that the largest and the smallest $m_W^{\rm MSSM} - m_W^{\rm SM}$ values are found in the external and central forbidden regions (both with $m_{h^0} < 122$ GeV) where we can appreciate the important influence that A_t has on the prediction of $m_W^{\rm MSSM}$ since if the value of A_t is increased the difference between the SM and the MSSM prediction of W boson mass will grow. A complete analysis of this plot will be given in Sec. 5.3.

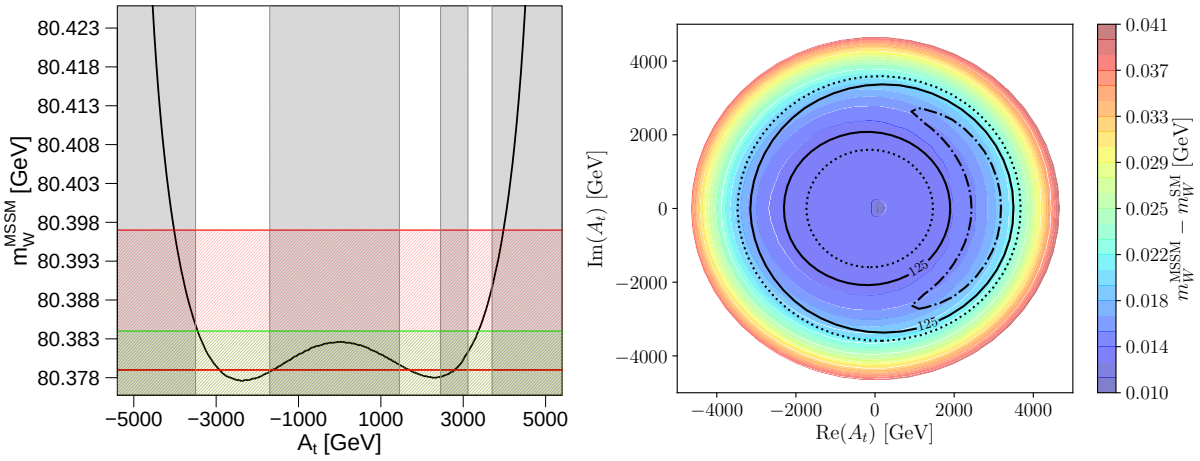

Figure 16: Dependence of m_W^{MSSM} on A_t (left) and the difference between the MSSM prediction m_W^{MSSM} and the SM prediction m_W^{SM} with the complex A_t plane (right). The gray area (left) denotes the forbidden region where $m_{h^0} \neq (125 \pm 3)$ GeV, the red area denotes the present uncertainty with the actual experimental value of the W boson mass and the green area denotes the future uncertainty with the actual experimental value of the W boson mass, see Tab. 3. The solid black line (right) denotes the value of $m_{h^0} = 125$ GeV and the dotted and dash-dotted lines denote the values of $m_{h^0} = 122$ GeV and $m_{h^0} = 128$ GeV, respectively. The rest of the MSSM parameters are set to the values in the $m_h^{\mathrm{mod+}}$ scenario (Tab. 4).

5.2 Dependence of m_W^{MSSM} on the squarks soft SUSY-breaking mass parameters

In this section we study how the soft SUSY-breaking mass parameters of squarks, $M_{\tilde{Q}_3}$ and $M_{\tilde{u}_3}$ (the plane $M_{\tilde{Q}_3} - M_{\tilde{u}_3}$), affect the mass of W boson m_W^{MSSM} and how much does it differs from the SM prediction m_W^{SM}.

In Fig. 17 we can see the difference between the MSSM and the SM prediction of the W boson mass $m_W^{\mathrm{MSSM}} - m_W^{\mathrm{SM}}$ with the plane $M_{\tilde{Q}_3} - M_{\tilde{u}_3}$ for $A_t = 1500$ GeV (left), $A_t = 2000$ GeV (right) and $A_t = 2500$ GeV (bottom). The solid black line denotes the value of $m_{h^0} = 125$ GeV and the dotted and dash-dotted lines denote the values of

$m_{h^0} = 122$ GeV and $m_{h^0} = 128$ GeV, respectively. First, for all plots in Fig. 17, it is important to highlight that the biggest difference between $m_W^{\rm MSSM}$ and $m_W^{\rm SM}$ is for small values of $M_{\tilde{Q}_3}$ and $M_{\tilde{u}_3}$ (within the allowed region). This is due to the stop/sbottom contribution to $\Delta\rho$ via the diagrams show in Fig. 5. Moreover, in the right and bottom plots of Fig. 17, these larger differences are found in the vicinity of the $m_{h^0} = 125$ GeV solid black line. So, if we increase the value of $M_{\tilde{Q}_3}$ and $M_{\tilde{u}_3}$ the difference between the SM and the MSSM prediction of W boson mass will decrease i.e. the third generation of squarks soft SUSY-breaking mass parameters increase the mass of the squarks so these particles do not have contribution and we recover the SM prediction.

At the left of Fig. 17 it is shown that the smallest $m_W^{\rm MSSM} - m_W^{\rm SM}$ values are found for large $M_{\tilde{Q}_3}$ and $M_{\tilde{u}_3}$ values and outside the allowed region (with $m_{h^0} < 122$ GeV) where this difference is around 8 MeV. The reason for this remaining differences, i.e. the fact that $m_W^{\rm MSSM} - m_W^{\rm SM}$ does not go to zero, are due to the rest of the SUSY spectrum, which is fixed, i.e. not moved to higher mass values. The largest differences can be found inside the allowed region ($M_{\tilde{Q}_3} = M_{\tilde{u}_3} > 700$ GeV) with $M_{\tilde{Q}_3}$ and $M_{\tilde{u}_3}$ values lower than 2000 GeV where $m_W^{\rm MSSM} - m_W^{\rm SM}$ is around 15 MeV for $M_{\tilde{Q}_3} = M_{\tilde{u}_3} \simeq 1800$ GeV and that difference is around 27 MeV for $M_{\tilde{Q}_3} = M_{\tilde{u}_3} \simeq 800$ GeV. In view of all the above, it is possible to see remarkable effects on the mass of W boson for values of $M_{\tilde{Q}_3}$ and $M_{\tilde{u}_3}$ below 1200 GeV with the precision at the current time. However, all the plane $M_{\tilde{Q}_3} - M_{\tilde{u}_3}$ studied shows observable effects in $m_W^{\rm MSSM}$ with the resolution at the future.

At the right and bottom of Fig. 17 (with $A_t = 2000$ GeV and $A_t = 2500$ GeV, respectively) we can see a similar behavior between both plots: the smallest $m_W^{\rm MSSM} - m_W^{\rm SM}$ values are found for large $M_{\tilde{Q}_3}$ and $M_{\tilde{u}_3}$ values where these differences are around 6 MeV and 4 MeV, respectively. On the other hand, the greater differences of $m_W^{\rm MSSM} - m_W^{\rm SM}$ are found within the region that surrounds the solid black line (at lower values of $M_{\tilde{Q}_3}$ and $M_{\tilde{u}_3}$) plus the allowed region at the lowest values of $M_{\tilde{Q}_3}$ and $M_{\tilde{u}_3}$, i.e. between $M_{\tilde{Q}_3} = M_{\tilde{u}_3} \simeq 800$ GeV and $M_{\tilde{Q}_3} = M_{\tilde{u}_3} \simeq 2000$ GeV for $A_t = 2000$ GeV and between $M_{\tilde{Q}_3} = M_{\tilde{u}_3} \simeq 1200$ GeV and $M_{\tilde{Q}_3} = M_{\tilde{u}_3} \simeq 3000$ GeV for $A_t = 2500$ GeV. In the first case (right), $m_W^{\rm MSSM} - m_W^{\rm SM}$ approximately changes 20 MeV and, in the second case (bottom), $m_W^{\rm MSSM} - m_W^{\rm SM}$ approximately changes 15 MeV as we can see in Fig. 17. Although these effects are not clearly measurable with the current accuracy, this region (in both plots) becomes very interesting with the future's resolution in order to detect an important change of $m_W^{\rm MSSM}$ and, with that, to constrain the space of the MSSM parameters.

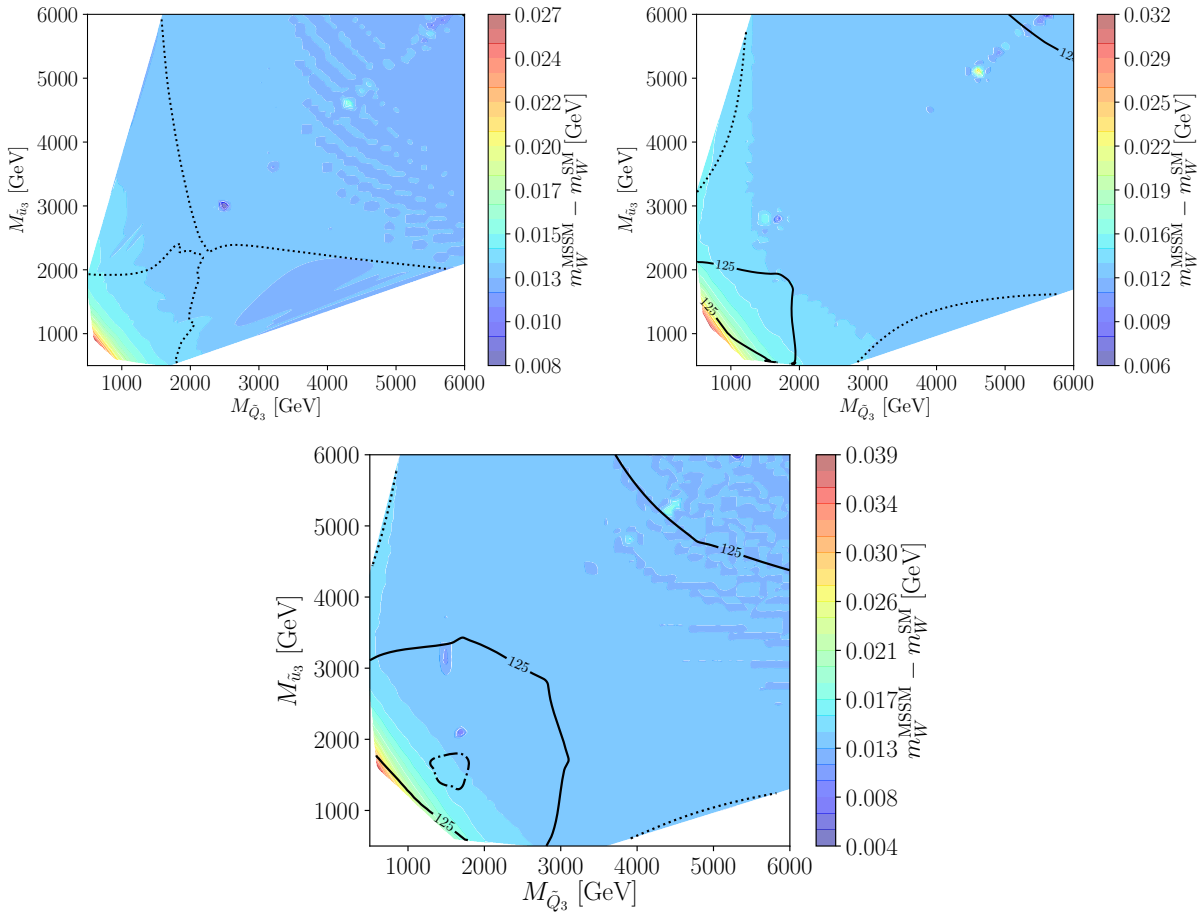

Figure 17: Dependence of the difference between the MSSM prediction $m_W^{\rm MSSM}$ and the SM prediction $m_W^{\rm SM}$ with the plane $M_{\tilde{Q}_3} - M_{\tilde{u}_3}$ for $A_t = 1500$ GeV (left), $A_t = 2000$ GeV (right) and $A_t = 2500$ GeV (bottom). The solid black line denotes the value of $m_{h^0} = 125$ GeV and the dotted and dash-dotted lines denote the values of $m_{h^0} = 122$ GeV and $m_{h^0} = 128$ GeV, respectively. The rest of the MSSM parameters are set to the values in the $m_h^{\rm mod+}$ scenario (Tab. 4).

5.3 Dependence of $m_W^{\rm MSSM}$ on the squarks soft SUSY-breaking mass parameters in the complex A_t plane

In this section we study how the complex plane of A_t affects the mass of W boson $m_W^{\rm MSSM}$ and how much does it differs from the SM prediction $m_W^{\rm SM}$ for different values of $M_{\tilde{Q}_3}$ and $M_{\tilde{u}_3}$ but with the requemirent that $M_{\tilde{Q}_3} = M_{\tilde{u}_3}$.

In Fig. 18 we can see the difference between the MSSM and the SM predictions of the W boson mass $m_W^{\rm MSSM} - m_W^{\rm SM}$ with the complex A_t plane with different values of $M_{\tilde{Q}_3}$ and $M_{\tilde{u}_3}$. First, for all the analyzed cases, it can be seen that the largest $m_W^{\rm MSSM} - m_W^{\rm SM}$ is found in the external forbidden region (with $m_{h^0} < 122$ GeV) and the smallest values of $m_W^{\rm MSSM} - m_W^{\rm SM}$ are found in the central forbidden region (with $|A_t| < 1800$ GeV and $m_{h^0} < 122$ GeV) of the complex plane of A_t. In particular, for the three cases that we have studied, the smallest difference between the MSSM and the SM predictions of the W boson mass is about 14 MeV. Moreover, we can see that the influence of A_t strongly affects the MSSM prediction since, as we can see in all plots of Fig. 18, the difference between the MSSM and the SM predictions is greater when more positive (or negative) is the value of A_t. In addition to that, if we analyze the influence of Φ_{A_t} (as wee can see in the right plot of Fig. 21, Appendix B) it can be seen that Φ_{A_t} practically does not affect the $m_W^{\rm MSSM}$ since the largest variation of $m_W^{\rm MSSM} - m_W^{\rm SM}$ is about 3 MeV (for $A_t = 3500$ GeV and $M_{\tilde{Q}_3} = M_{\tilde{u}_3} = 1500$ GeV) which is far from the best precision value of $m_W^{\rm MSSM}$ that it is expected at the future. So, it is not possible to get valid information from $m_W^{\rm MSSM}$ on the phase of A_t.

At the left of Fig. 18 we can see, in the allowed region (in the real A_t line, from $A_t = 1500$ GeV to $A_t = 2500$ GeV, $A_t = 3000$ GeV to $A_t = 3500$ GeV and from $A_t = -1500$ GeV to $A_t = -3000$ GeV), the difference between the MSSM and the SM predictions increases with the value of $|A_t|$ to the limit of the allowed region from $m_W^{\rm MSSM} - m_W^{\rm SM} \simeq 14$ MeV to $m_W^{\rm MSSM} - m_W^{\rm SM} \simeq 23$ MeV. These changes within the allowed region are remarkable because with the present (with $A_t > 3000$ GeV) and the future resolution these effects in the mass of the W boson can be observable. At the right of Fig. 18 we can see within the allowed region (in the real A_t line, from $A_t = 1500$ GeV to $A_t = 3000$ GeV, from $A_t = 4500$ GeV to $A_t = 5000$ GeV and $A_t = -1500$ GeV to $A_t = -4500$ GeV) the difference between the MSSM and the SM predictions increases with the value of $|A_t|$ to the limit of the allowed region from $m_W^{\rm MSSM} - m_W^{\rm SM} \simeq 14$ MeV to $m_W^{\rm MSSM} - m_W^{\rm SM} \simeq 19$ MeV. Finally, at the bottom of Fig. 18 we can see (the allowed region mainly includes the real A_t line from $A_t = 1500$ GeV to $A_t = 3000$ GeV, from $A_t = 5500$ GeV to $A_t = 6250$ GeV, from $A_t = -1500$ GeV to $A_t = -3500$ GeV and from $A_t = -4500$ GeV to $A_t = -5750$ GeV) the difference between the MSSM and the SM predictions increases with the value of $|A_t|$ to the limit of the allowed region from

$m_W^{\rm MSSM} - m_W^{\rm SM} \simeq 14$ MeV to $m_W^{\rm MSSM} - m_W^{\rm SM} \simeq 17$ MeV. Unlike to the previous case, these effects only can be observable with the future precision in the mass of the W boson for both cases. The present resolution does not show valid information about these cases according to the value of $m_W^{\rm MSSM}$.

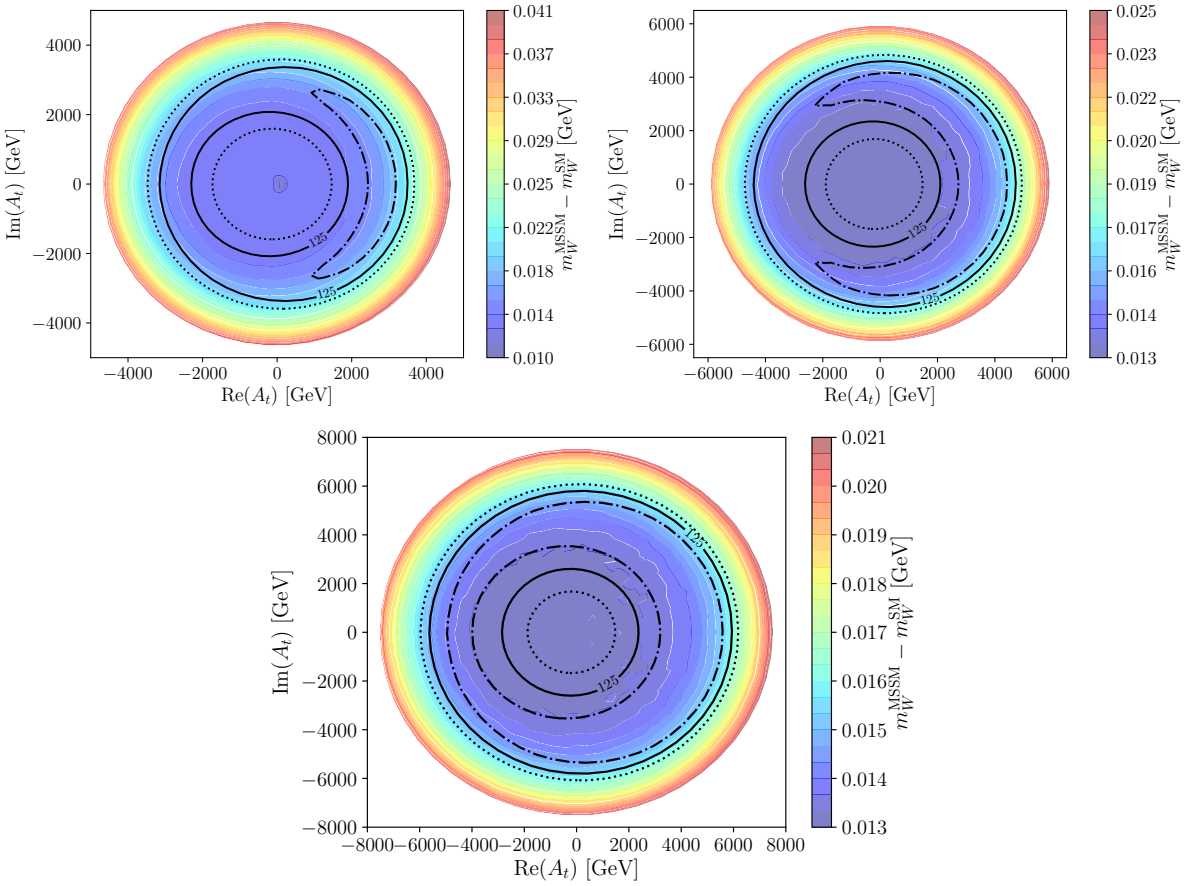

Figure 18: Dependence of the difference between the MSSM prediction $m_W^{\rm MSSM}$ and the SM prediction $m_W^{\rm SM}$ in the complex A_t with $M_{\tilde{Q}_3} = M_{\tilde{u}_3} = 1500$ GeV (left), $M_{\tilde{Q}_3} = M_{\tilde{u}_3} = 2000$ GeV (right) and $M_{\tilde{Q}_3} = M_{\tilde{u}_3} = 2500$ GeV (bottom). The solid black line denotes the value of $m_{h^0} = 125$ GeV and the dotted and dash-dotted lines denote the values of $m_{h^0} = 122$ GeV and $m_{h^0} = 128$ GeV, respectively. The rest of the MSSM parameters are set to the values in the $m_h^{\rm mod+}$ scenario (Tab. 4).

Based on all the above, it can be concluded that, as we saw in Sec. 5.1, A_t strongly and positively contributes in the MSSM prediction of the W boson mass and, in addition to that, only when the value of the soft SUSY-breaking parameters $M_{\tilde{Q}_3}$ and $M_{\tilde{u}_3}$ are not very large, as we saw in Sec. 5.2, we can observe detectable effects on the $m_W^{\rm MSSM}$ which has been completed with the analysis discussed in this section.

5.4 Dependence of $m_W^{\rm MSSM}$ on the sleptons soft SUSY-breaking mass parameters

In this section we study how the soft SUSY-breaking mass parameters of the third generation of sleptons $M_{\tilde{X}_3}$ (with $\tilde{X} = \tilde{L}, \tilde{e}$) affect the mass of W boson $m_W^{\rm MSSM}$ and how much does it differs from the SM prediction $m_W^{\rm SM}$.

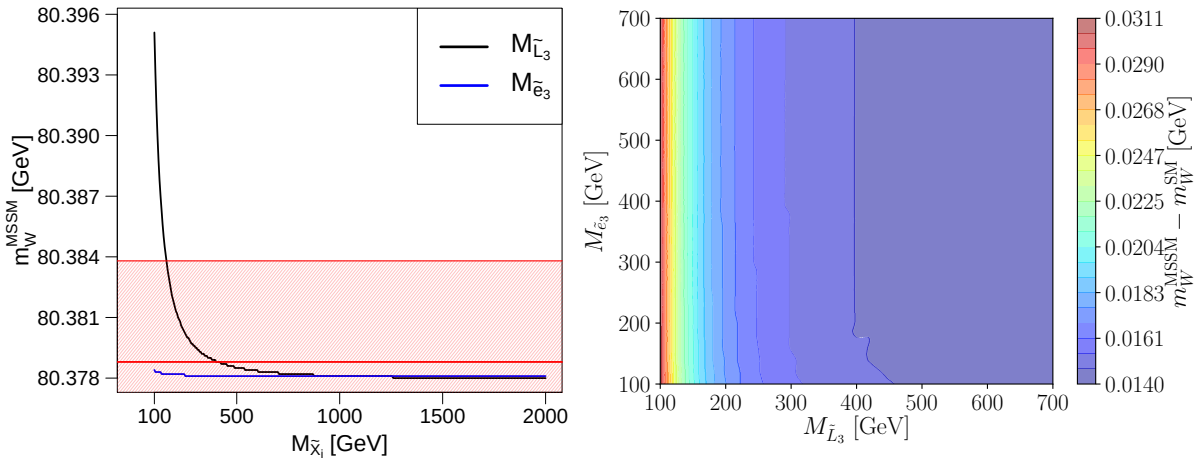

Figure 19: Dependence of $m_W^{\rm MSSM}$ with the sleptons soft SUSY-breaking mass (left) and the difference between the MSSM prediction $m_W^{\rm MSSM}$ and the SM prediction $m_W^{\rm SM}$ with the plane $M_{\tilde{L}_3} - M_{\tilde{e}_3}$ (right). The red area (left) denotes the future uncertainty with the actual experimental value of the W boson mass $m_W^{\rm fut} = (80.379 \pm 0.005)$ GeV (The present uncertainty fills all the space studied). The rest of the MSSM parameters are set to the values in the $m_h^{\rm mod+}$ scenario (Tab. 4).

In Fig. 19 it is shown the dependence of the mass of W boson with different values of $M_{\tilde{L}_3}$ and $M_{\tilde{e}_3}$ (left) and the difference between the MSSM and the SM prediction of the

W boson mass $m_W^{\rm MSSM} - m_W^{\rm SM}$ with the plane $M_{\tilde{L}_3} - M_{\tilde{e}_3}$ (right). In addition to that, as we can see in Fig. 15, all the $M_{\tilde{X}_3}$ (with $\tilde{X} = \tilde{L}, \tilde{e}$) space that we have scanned it is within the allowed region for m_{h^0}. First, in the left plot of Fig. 19 we can see a strong positive influence of $M_{\tilde{L}_3}$ with the mass of W i.e. the mass of $m_W^{\rm MSSM}$ decreases with the increase of $M_{\tilde{L}_3}$ to $M_{\tilde{L}_3} \simeq 700$ GeV from which the mass of W boson remains constant for large values of $M_{\tilde{L}_3}$. Moreover, the most important change of $m_W^{\rm MSSM}$ (in the range 100 GeV $\leq M_{\tilde{L}_3} \leq$ 160 GeV) will be able to detect with the future's precision since the variation of $m_W^{\rm MSSM}$ is about 13 MeV within this range. On the other hand, the influence of $M_{\tilde{e}_3}$ with the mass of W boson is practically negligible (it is around 1 MeV). Note that, for $M_{\tilde{L}_3} = M_{\tilde{e}_3} > 700$ GeV, $m_W^{\rm MSSM}$ is constant and equal according to both SUSY-breaking parameters.

Finally, in the right plot of Fig. 19 we show the dependence of $m_W^{\rm MSSM} - m_W^{\rm SM}$ with the plane $M_{\tilde{L}_3} - M_{\tilde{e}_3}$. We can see that the biggest difference between $m_W^{\rm MSSM}$ and $m_W^{\rm SM}$ is for small values of $M_{\tilde{L}_3}$ and any value $M_{\tilde{e}_3}$ (since its influence is negligible) where this difference can be as large as 31 MeV. Note that this strong effect on $m_W^{\rm MSSM}$ is within the current resolution for the measurement of the mass of the W boson i.e. in other words, a persistent discrepancy between $m_W^{\rm exp}$ and $m_W^{\rm SM}$ could be explained by the presence of very light staus alone. In addition to that, as the value of $M_{\tilde{L}_3}$ is increased that difference betweeen both predictions decreases to $M_{\tilde{L}_3}$ reaches a value of $\simeq 400$ GeV where $m_W^{\rm MSSM} - m_W^{\rm SM}$ is almost constante and its value is approximately 14 MeV which is only measurable with the future's resolution. So, small values of $M_{\tilde{L}_3}$ positively affect the MSSM prediction $m_W^{\rm MSSM}$ and this contribution decreases according as its value increases.

In summary, as we saw in Sec. 2.4, these parameters affect directly at the W boson sector in the MSSM. With this numerical analysis it has been determined the most relevant ranges of MSSM parameters that produce a measurable effect on the mass of the W boson $m_W^{\rm MSSM}$. These results are collected in the Tab. 5 which is shown in the next section.

6 Conclusions

In this work it has been scanned the MSSM space of parameters in order to analyze the W boson sector within of this model. First, we have briefly explained the SM and what are the problems that this model has. Based on it, we have presented the MSSM and it has been explained how this model solves the SM problems. Second, we have briefly discussed the $m_h^{\text{mod+}}$ scenario and we have studied the dependence of the mass of h^0 with the MSSM parameters within this scenario in order to get the range of these parameters which m_{h^0} is inside the region of phenomenological validity (i.e. $m_{h^0} = (125 \pm 3)$ GeV) in accordance with the experimental datas. Finally, in the allowed region given by the mass of h^0, we have analyzed the space of MSSM parameters in order to find those for which m_W^{MSSM} is more sensitive and, with that, to constrain the parameters space. In view of all the above, the analysis realized in this master thesis has provided the following conclusions:

- The trilinear Higgs-stop coupling A_t has a very important effect on the mass of h^0 but it only shows three limited regions which provide a h^0 with mass in agreement with the region of phenomenological validity. The rest of MSSM parameters analyzed also have influence but this almost always within the theoretical uncertainty of ± 3 GeV.

- All the MSSM parameters scanned have a detectable impact on m_W^{MSSM} when they take their lower values (except A_t which increases the difference between the MSSM and the SM predictions as A_t increases), i.e where we expect that SUSY has an measurable influence. These effects on m_W^{MSSM} limit the values that the MSSM parameters can take (as we summarized in Tab. 5). In the future, with more accurate resolution, it is expected to measure a small variation in W boson mass that indicates what is the range of values of these MSSM parameters.

- In particular, if we consider that the present discrepancy between m_W^{exp} and m_W^{SM} is the same at the future, we can explain that discrepancy due to the contribution of very light staus alone.

- The Higgs boson mass is very sensitive to new physics i.e m_{h^0} is very influenced for the value of the other MSSM parameters. To get more theoretical precision in the prediction would allow us to repeat this analysis in a more exhaustive way.

Finally, in Tab. 5 are colleted all the results shown in Sec. 5 i.e. the ranges of MSSM parameters scanned (in the $m_h^{\text{mod+}}$ scenario) that produce a measurable effect on the mass of the m_W^{MSSM} with the present resolution and the future precision that is expected on the mass of W boson.

Time	A_t (Real line)	$M_{\tilde{Q}_3} - M_{\tilde{u}_3}$ ($A_t = 1500$ GeV)	$M_{\tilde{Q}_3} - M_{\tilde{u}_3}$ ($A_t = 2000$ GeV)	$M_{\tilde{Q}_3} - M_{\tilde{u}_3}$ ($A_t = 2500$ GeV)
Present	$-$	$-$	$-$	$-$
Future	$3115 - 3700$	$\{700 - 2000\}$	$\{800 - 2000\}$	$\{1200 - 3000\}$

Time	Complex A_t ($M_{\tilde{Q}_3} = M_{\tilde{u}_3} = 1500$ GeV)	Complex A_t ($M_{\tilde{Q}_3} = M_{\tilde{u}_3} = 2000$ GeV)
Present	$3000 - 3500$	$-$
Future	$\begin{cases} (-1500) - (-3000) \\ 1500 - 2500 \\ 3000 - 3500 \end{cases}$	$\begin{cases} (-1500) - (-4500) \\ 1500 - 3000 \\ 4500 - 5000 \end{cases}$

Time	Complex A_t ($M_{\tilde{Q}_3} = M_{\tilde{u}_3} = 2500$ GeV)	$M_{\tilde{L}_3}$ ($A_t = 2000$ GeV)	$M_{\tilde{L}_3} - M_{\tilde{e}_3}$ ($A_t = 2000$ GeV)
Present	$-$	$-$	$(100 - 400) - (100 - 700)$
Future	$\begin{cases} (-1500) - (-3500) \\ (-4500) - (-5750) \\ 1500 - 3000 \\ 5500 - 6250 \end{cases}$	$100 - 160$	$\{100 - 700\}$

Table 5: Ranges of the MSSM parameters that produce a measurable effect on m_W^{MSSM} with the present and future resolution. The value between braces (when we study the planes $M_{\tilde{Q}_3} - M_{\tilde{u}_3}$ and $M_{\tilde{L}_3} - M_{\tilde{e}_3}$) correspond with the range for both parameters.

Appendix A Dependence of m_{h^0} with the stau and sbottom couplings

In Fig. 20 we show the variation of the mass of h^0 as a function of trilinear Higgs-sbottoms coupling A_b (left) and trilinear Higgs-staus coupling A_τ (right).

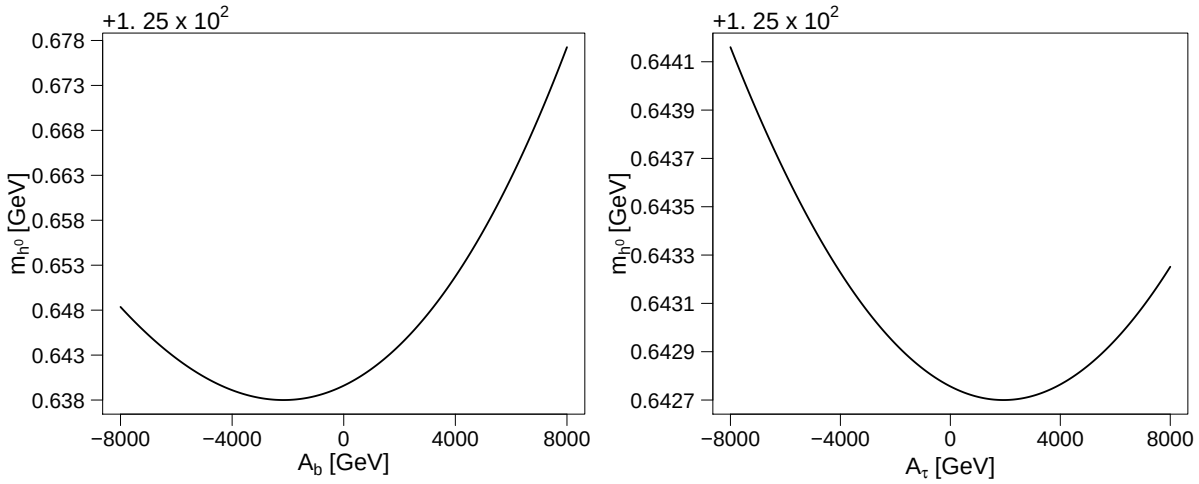

Figure 20: Dependence of m_{h^0} with A_b (left) and A_τ (right). The rest of the MSSM parameters are set to the values in the $m_h^{\text{mod+}}$ scenario (Tab. 4).

In both plots we can see that the change in the mass of h^0 is practically negligible for large values of A_b and A_τ (-8 TeV $< A_b,\ A_\tau < 8$ TeV). As we can see in Eq.(53), the mass of h^0 are proportional to m_t^4, m_b^4 and m_τ^4 in each respective sector. Compared with the mass of top m_t, the mass of bottom and tau (m_b and m_τ, respectively) are light and this is the principal reason that explains this small dependence between m_h^0 with the sbottom and stop couplings.

Appendix B Other dependences of $m_W^{\rm MSSM}$

In this appendix we show how much does the W boson $m_W^{\rm MSSM}$ differs from the SM prediction $m_W^{\rm MSSM} - m_W^{\rm SM}$ as function of the module (left) and the phase of A_t (right) with $|A_t| = 3500$ GeV and the $M_{\rm SUSY}$ parameter (bottom) i.e. how these parameters affect the mass of the W boson $m_W^{\rm MSSM}$ for $M_{\tilde{Q}_3} = M_{\tilde{u}_3} = 1500$ GeV inside the allowed region for the mass of h^0.

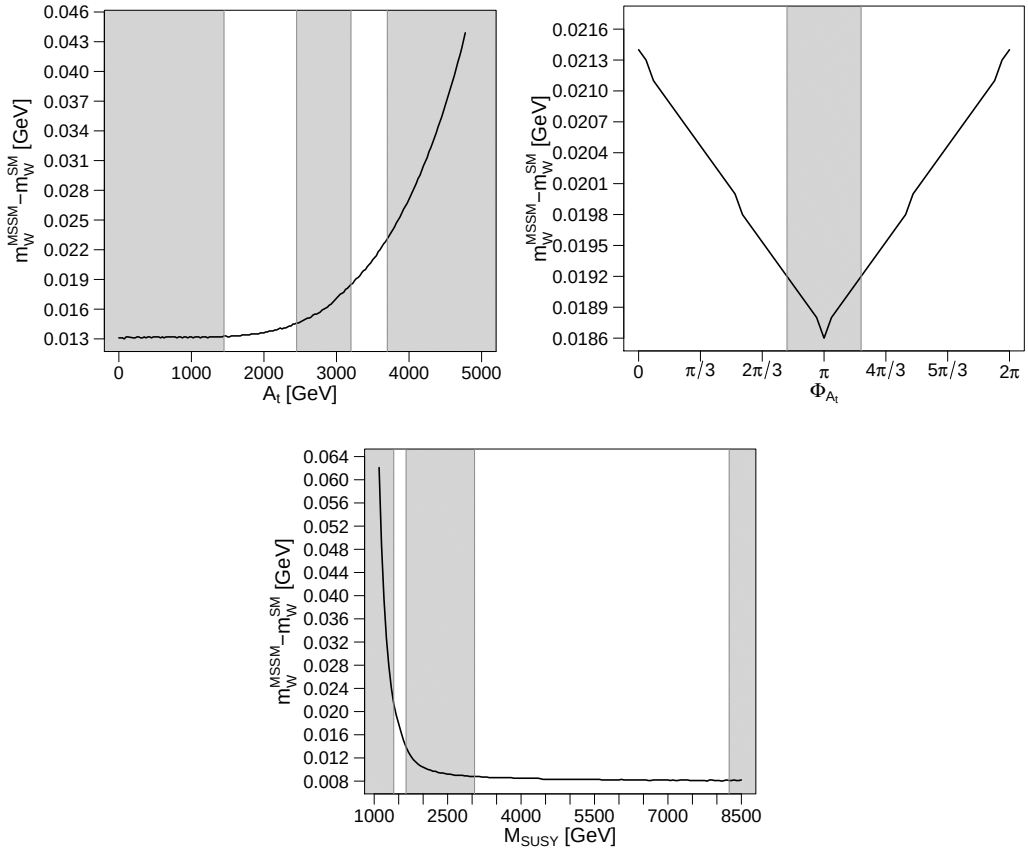

Figure 21: Dependence of the difference between the MSSM prediction $m_W^{\rm MSSM}$ and the SM prediction $m_W^{\rm SM}$ in the complex A_t (left and right) and with the $M_{\rm SUSY}$ parameter (bottom) for $M_{\tilde{Q}_3} = M_{\tilde{u}_3} = 1500$ GeV. The grey area denotes the forbidden region where $m_{h^0} \neq (125 \pm 3)$ GeV. The rest of the MSSM parameters are set to the values in the $m_h^{\rm mod+}$ scenario (Tab. 4).

References

[1] S. Chatrchyan *et. al* [CMS Collaboration]. Observation of a new boson at a mass of 125 GeV with the CMS experiment at the LHC. *Physics Letters B*, 716(1):30–61, 2012.

[2] G. Aad *et. al* [ATLAS Collaboration]. Observation of a new particle in the search for the Standard Model Higgs boson with the ATLAS detector at the LHC. *Physics Letters B*, 716(1):1–29, 2012.

[3] H. P. Nilles. Supersymmetry, supergravity and particle physics. *Physics Reports*, 110(1-2):1–162, 1984.

[4] H. E. Haber and G. L. Kane. The search for supersymmetry: probing physics beyond the Standard Model. *Physics Reports*, 117(2-4):75–263, 1985.

[5] R. Barbieri. Looking beyond the Standard Model: the supersymmetric option. *La Rivista del Nuovo Cimento (1978-1999)*, 11(4):1–45, 1988.

[6] A. Bilal. Introduction to supersymmetry. *arXiv preprint hep-th/0101055*, 2001.

[7] CMS collaboration. CMS Supersymmetry Physics Results. `https://twiki.cern.ch/twiki/bin/view/CMSPublic/PhysicsResultsSUS`.

[8] ATLAS SUSY Working Group. ATLAS experiment - Supersymmetry searches public results. `https://twiki.cern.ch/twiki/bin/view/AtlasPublic/SupersymmetryPublicResults`.

[9] Georges Aad, B Abbott, J Abdallah, O Abdinov, R Aben, M Abolins, OS AbouZeid, H Abramowicz, H Abreu, R Abreu, et al. Combined Measurement of the Higgs Boson Mass in pp Collisions at $\sqrt{s} = 7$ and 8 TeV with the ATLAS and CMS Experiments. *Physical review letters*, 114(19):191803, 2015.

[10] G. Degrassi, S. Heinemeyer, W. Hollik, P. Slavich, and G. Weiglein. Towards high-precision predictions for the MSSM Higgs sector. *The European Physical Journal C-Particles and Fields*, 28(1):133–143, 2003.

[11] J. Haller, A. Hoecker, R. Kogler, K. Mönig, T. Peiffer, and J. Stelzer. Update of the global electroweak fit and constraints on two-Higgs-doublet models. *arXiv preprint arXiv:1803.01853*, 2018.

[12] Mark Thomson. *Modern particle physics*. Cambridge University Press, New York, 2013.

[13] E. Rutherford F.R.S. The scattering of α and β particles by matter and the structure of the atom. *Philosophical Magazine*, 92(4):379–398, 1911.

[14] E. Rutherford F.R.S. LIV. Collision of α particles with light atoms. IV. An anomalous effect in nitrogen. *The London, Edinburgh, and Dublin Philosophical Magazine and Journal of Science*, 37(222):581–587, 1919.

[15] J. Chadwick. The existence of a neutron. *Proceedings of the Royal Society of London A: Mathematical, Physical and Engineering Sciences*, 136(830):692–708, 1932.

[16] E. D. Bloom, D. H. Coward, H. DeStaebler, J. Drees, G. Miller, L. W. Mo, R. E. Taylor, M. Breidenbach, J. I. Friedman, G. C. Hartmann, and H. W. Kendall. High-Energy Inelastic $e - p$ Scattering at 6^o and 10^o. *Phys. Rev. Lett.*, 23:930–934, Oct 1969.

[17] M. Breidenbach, J. I. Friedman, H. W. Kendall, E. D. Bloom, D. H. Coward, H. DeStaebler, J. Drees, L. W. Mo, and R. E. Taylor. Observed Behavior of Highly Inelastic Electron-Proton Scattering. *Phys. Rev. Lett.*, 23:935–939, Oct 1969.

[18] Steven Weinberg. *The quantum theory of fields. Vol. 1: Foundations.* Cambridge University Press, 1995.

[19] M. Tanabashi *et. al* [Particle Data Group]. Review of Particle Physics. *Phys. Rev. D*, 98:030001, Aug 2018.

[20] M. Drewes. The phenomenology of right handed neutrinos. *International Journal of Modern Physics E*, 22(08):1330019, 2013.

[21] The United States at the LHC. The Standard Model and beyond. `http://united-states.cern/physics/standard-model-and-beyond`.

[22] F. Englert and R. Brout. Broken Symmetry and the Mass of Gauge Vector Mesons. *Phys. Rev. Lett.*, 13:321–323, Aug 1964.

[23] P. W. Higgs. Broken Symmetries and the Masses of Gauge Bosons. *Phys. Rev. Lett.*, 13:508–509, Oct 1964.

[24] M. von Steinkirch. Introduction to group theory for physicists. 2011.

[25] S. L. Glashow. The renormalizability of vector meson interactions. *Nuclear Physics*, 10:107 – 117, 1959.

[26] A. Salam and J. C. Ward. Weak and electromagnetic interactions. *Il Nuovo Cimento (1955-1965)*, 11(4):568–577, Feb 1959.

[27] S. Weinberg. A Model of Leptons. *Phys. Rev. Lett.*, 19:1264–1266, Nov 1967.

[28] K. Nishijima. Charge Independence Theory of V Particles. *Progress of Theoretical Physics*, 13(3):285–304, 1955.

[29] M. Gell-Mann. The interpretation of the new particles as displaced charge multiplets. *Il Nuovo Cimento (1955-1965)*, 4(2):848–866, Apr 1956.

[30] P. Scott. Searches for Particle Dark Matter: an Introduction. *arXiv preprint arXiv:1110.2757*, 2011.

[31] T. Clifton, P. G. Ferreira, A. Padilla, and C. Skordis. Modified gravity and cosmology. *Physics Reports*, 513(1):1 – 189, 2012. Modified Gravity and Cosmology.

[32] J.G. De Swart, G. Bertone, and J. van Dongen. How dark matter came to matter. *Nature Astronomy*, 1(3):0059, 2017.

[33] H. Georgi and S. L. Glashow. Unity of All Elementary-Particle Forces. *Phys. Rev. Lett.*, 32:438–441, Feb 1974.

[34] H. Hatanaka, T. Inami, and C.S. Lim. The Gauge Hierarchy Problem and Higher-Dimensional Gauge Theories. *Modern Physics Letters A*, 13(32):2601–2611, 1998.

[35] M. Planck. Naturlische masseinheiten. *Der Köniqlich Preussischen Akademie Der Wissenschaften*, page 479, 1899.

[36] J. D. Bekenstein. Black Holes and Entropy. *Phys. Rev. D*, 7:2333–2346, Apr 1973.

[37] M. Drees, R. Godbole, and P. Roy. *Theory and Phenomenology of Sparticles*. World Scientific, 2005.

[38] Supergauge transformations in four dimensions. *Nuclear Physics B*, 70(1):39 – 50, 1974.

[39] S. P. Martin. A supersymmetry primer. In *Perspectives on supersymmetry II*, pages 1–153. World Scientific, 2010.

[40] L. Girardello and M.T. Grisaru. Soft breaking of supersymmetry. *Nuclear Physics B*, 194(1):65 – 76, 1982.

[41] SP Martin. A supersymmetry primer (hep-ph/9709356) preprint martin sp 1998. *Adv. Ser. Direct. High Energy Phys*, 18(1), 1997.

[42] P. Draper and H. Rzehak. A review of Higgs mass calculations in supersymmetric models. *Physics Reports*, 619:1–24, 2016.

[43] M. Gomez-Bock, M. Mondragon, M. Mühlleitner, M. Spira, and P.M. Zerwas. Concepts of electroweak symmetry breaking and Higgs physics. *arXiv preprint arXiv:0712.2419*, 2007.

[44] A. Dobado, M.J. Herrero, and S. Penaranda. The Higgs sector of the MSSM in the decoupling limit. *The European Physical Journal C-Particles and Fields*, 17(3):487–500, 2000.

[45] S. Heinemeyer, W. Hollik, and G. Weiglein. The mass of the lightest MSSM Higgs boson: A compact analytical expression at the two-loop level. *Physics Letters B*, 455(1-4):179–191, 1999.

[46] S. Heinemeyer, W. Hollik, and G. Weiglein. The masses of the neutral CP-even Higgs bosons in the MSSM: Accurate analysis at the two-loop level. *The European Physical Journal C-Particles and Fields*, 9(2):343–366, 1999.

[47] R.-J. Zhang. Two-loop effective potential calculation of the lightest CP-even Higgs-boson mass in the MSSM. *Physics Letters B*, 447(1-2):89–97, 1999.

[48] I. JR. Aitchison. Supersymmetry and the MSSM: An elementary introduction. *arXiv preprint hep-ph/0505105*, 2005.

[49] M. Frank, T. Hahn, S. Heinemeyer, W. Hollik, H. Rzehak, and G. Weiglein. The Higgs boson masses and mixings of the complex MSSM in the Feynman-diagrammatic approach. *Journal of High Energy Physics*, 2007(02):047, 2007.

[50] R. Dermisek and I. Low. Probing the Stop Sector of the MSSM with the Higgs Boson at the LHC. *arXiv preprint hep-ph/0701235*, 2007.

[51] S. Jung and J. D. Wells. Gaugino physics of split supersymmetry spectra at the LHC and future proton colliders. *Physical Review D*, 89(7):075004, 2014.

[52] M. Mühlleitner, H. Rzehak, and M. Spira. MSSM Higgs boson production via gluon fusion: the large gluino mass limit. *Journal of High Energy Physics*, 2009(04):023, 2009.

[53] S. K. Vempati. Introduction to MSSM. *arXiv preprint arXiv:1201.0334*, 2012.

[54] M. Boz and N. K. Pak. The neutralino mass: correlation with the charginos. *Modern Physics Letters A*, 21(20):1609–1623, 2006.

[55] S. Y Choi, B. Chung, P. Ko, and J. Lee. CP–violating Chargino Contributions to the Higgs Coupling to Photon Pairs in the Decoupling Regime of Higgs Sector. *Physical Review D*, 66, 06 2002.

[56] Rabindra N Mohapatra. Supersymmetry and R-parity: an overview. *Physica Scripta*, 90(8):088004, 2015.

[57] R. F. Glennys and F. Pierre. Phenomenology of the production, decay, and detection of new hadronic states associated with supersymmetry. *Physics Letters B*, 76(5):575 – 579, 1978.

[58] J. Ellis and K. A. Olive. Supersymmetric dark matter candidates. *arXiv preprint arXiv:1001.3651*, 2010.

[59] A. M. Sirunyan *et. al* [CMS Collaboration]. Combined search for electroweak production of charginos and neutralinos in proton-proton collisions at $\sqrt{s} = 13$ TeV. *Journal of High Energy Physics*, 2018(3):160, 2018.

[60] S. Dedes, A. Heinemeyer, S. Su, and G. Weiglein. The lightest Higgs boson of mSUGRA, mGMSB and mAMSB at present and future colliders: observability and precision analyses. *Nuclear Physics B*, 674(1-2):271–305, 2003.

[61] Supersymmetry on the run: LHC and dark matter, author=Kazakov, D.I. *Nuclear Physics B-Proceedings Supplements*, 203:118–154, 2010.

[62] D.M. Webber, V. Tishchenko, Q. Peng, S. Battu, R.M. Carey, D.B. Chitwood, J. Crnkovic, P.T. Debevec, S. Dhamija, W. Earle, et al. Measurement of the positive muon lifetime and determination of the fermi constant to part-per-million precision. *Physical review letters*, 106(4):041803, 2011.

[63] S. Heinemeyer, W. Hollik, D. Stöckinger, A. M. Weber, and G. Weiglein. Precise prediction for MW in the MSSM. *Journal of High Energy Physics*, 2006(08):052, 2006.

[64] S. M. Berman. Radiative Corrections to Muon and Neutron Decay. *Phys. Rev.*, 112:267–270, Oct 1958.

[65] T. Kinoshita and A. Sirlin. Radiative Corrections to Fermi Interactions. *Phys. Rev.*, 113:1652–1660, Mar 1959.

[66] S. M. Berman and A. Sirlin. Some considerations on the radiative corrections to muon and neutron decay. *Annals of Physics*, 20(1):20–43, 1962.

[67] S. Heinemeyer, W. Hollik, G. Weiglein, and L. Zeune. Implications of LHC search results on the W boson mass prediction in the MSSM. *Journal of High Energy Physics*, 2013(12):84, 2013.

[68] V. Tishchenko *et. al.* Detailed report of the MuLan measurement of the positive muon lifetime and determination of the Fermi constant. *Phys. Rev. D*, 87:052003, Mar 2013.

[69] M. Baak, A. Blondel, A. Bodek, R. Caputo, T. Corbett, C. Degrande, O. Eboli, J. Erler, B. Feigl, A. Freitas, et al. Study of electroweak interactions at the energy frontier. *arXiv preprint arXiv:1310.6708*, 2013.

[70] M. Awramik, M. Czakon, A. Freitas, and G. Weiglein. Precise prediction for the W-boson mass in the Standard Model. *Physical Review D*, 69(5):053006, 2004.

[71] A. Freitas. Electroweak precision tests in the LHC era and Z-decay form factors at two-loop level. *arXiv preprint arXiv:1406.6980*, 2014.

[72] J. Haestier, D. Stöckinger, G. Weiglein, and S. Heinemeyer. Two-loop contributions to electroweak precision observables in the MSSM. *arXiv preprint hep-ph/0506259*, 2005.

[73] J. Haestier, S. Heinemeyer, D. Stöckinger, and G. Weiglein. Electroweak precision observables: Two-loop yukawa corrections of supersymmetric particles. *Journal of High Energy Physics*, 2005(12):027, 2005.

[74] G. Moortgat-Pick *et. al.* Physics at the e^+ e^- linear collider. *European Physical Journal C*, 75(8), 8 2015.

[75] S. S. AbdusSalam, B. C. Allanach, H. K. Dreiner, J. Ellis, U. Ellwanger, J. Gunion, S. Heinemeyer, M. Krämer, M. Mangano, K. A. Olive, S. Rogerson, L. Roszkowski, M. Schlaffer, and G. Weiglein. Benchmark models, planes, lines and points for future SUSY searches at the LHC. *The European Physical Journal C*, 71(12):1835, Dec 2011.

[76] M. Carena, S. Heinemeyer, O. Stål, CEM. Wagner, and G. Weiglein. MSSM Higgs boson searches at the LHC: benchmark scenarios after the discovery of a Higgs-like particle. *The European Physical Journal C*, 73(9):2552, 2013.

[77] CMS Collaboration et al. Search for additional neutral MSSM Higgs bosons in the $\tau\tau$ final state in proton-proton collisions at $\sqrt{s} = 13$ TeV. *arXiv preprint arXiv:1803.06553*, 2018.

[78] CMS Collaboration. Exclusion limits on gluino and top-squark pair production in natural SUSY scenarios with inclusive razor and exclusive single-lepton searches at 8 TeV. (CMS-PAS-SUS-14-011), 2014.

[79] H. Bahl, T. Hahn, S. Heinemeyer, Wolfgang Hollik, S. Paßehr, H. Rzehak, and G. Weiglein. Precision calculations in the MSSM Higgs-boson sector with FeynHiggs 2.14. 2018.

[80] S. Heinemeyer, W. Hollik, and G. Weiglein. FeynHiggs: a program for the calculation of the masses of the neutral CP-even Higgs bosons in the MSSM. *Computer Physics Communications*, 124(1):76–89, 2000.

[81] T. Hahn, S. Heinemeyer, W. Hollik, H. Rzehak, and G. Weiglein. High-Precision Predictions for the Light C P-Even Higgs Boson Mass of the Minimal Supersymmetric Standard Model. *Physical review letters*, 112(14):141801, 2014.

[82] H. Bahl and W. Hollik. Precise prediction for the light MSSM Higgs-boson mass combining effective field theory and fixed-order calculations. *The European Physical Journal C*, 76(9):499, 2016.

[83] H. Bahl, S. Heinemeyer, W. Hollik, and G. Weiglein. Reconciling EFT and hybrid calculations of the light MSSM Higgs-boson mass. *The European Physical Journal C*, 78(1):57, 2018.

[84] C. Han, J. Ren, L. Wu, J. M. Yang, and M. Zhang. Top-squark in natural SUSY under current LHC Run-2 data. *The European Physical Journal C*, 77(2):93, 2017.

[85] G. Aad *et. al* [ATLAS Collaboration]. Search for Scalar Bottom Quark Pair Production with the ATLAS Detector in pp Collisions at $\sqrt{s} = 7$ TeV. *Phys. Rev. Lett.*, 108:181802, May 2012.

[86] A. Heister *et. al.* Absolute Lower Limits on the Masses of Selectrons and Sneutrinos in the MSSM. 11 2018.

[87] P. Draper, G.l Lee, and C. E.M. Wagner. Precise estimates of the Higgs mass in heavy supersymmetry. *Physical Review D*, 89(5):055023, 2014.